Bogoliubov Laboratory of Theoretical Physics

JINR

Dubna, 25 September 2019

Joint Institute for Nuclear Research

SCIENCE BRINGING NATIONS TOGETHER

Investigating relativistic proton-nucleus collisions and the influence of electromagnetic fields on final hadronic observables

Lucia Oliva

Collaborators:

Elena Bratkovskaya, Pierre Moreau, Vadim Voronyuk

Helmholtzzentrum für Schwerionenforschung GmbH

GOETHE UNIVERSITÄT FRANKFURT AM MAIN

CRC-TR 211 Strong-interaction matter under extreme conditions

Alexander von Humboldt Stiftung/Foundation

Dynamics of quarks and gluons described by the Quantum Chromodynamics (QCD)

$$\mathcal{L}_{cl} = \bar{q}_i^{\alpha}\,(i\gamma^{\mu} D_{\mu} - m)^{ij}_{\alpha\beta}\, q_j^{\beta} - \frac{1}{4} F^a_{\mu\nu} F^{\mu\nu}_a$$

QCD LAGRANGIAN

QCD predicts that at very high energy quarks and gluons became weekly interacting

QUARK-GLUON PLASMA (QGP)

Collins and Perry, PRL 34 (1975) 1353

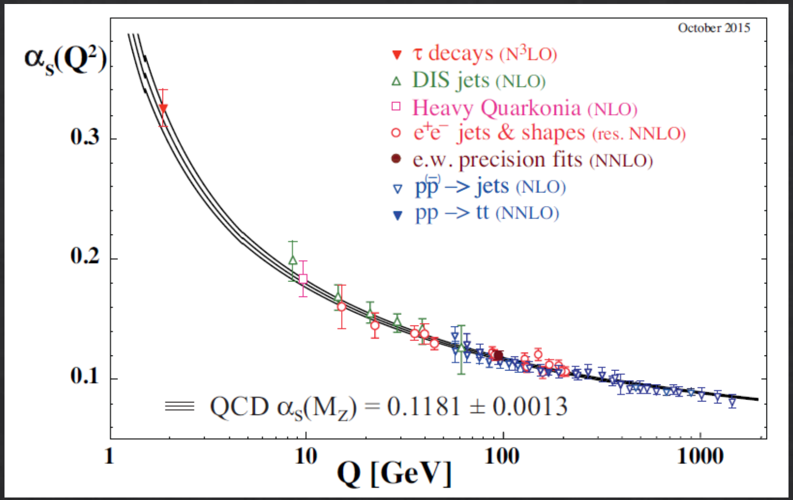

PDG, Chin. Phys. C 38, 010009 (2014-2015)

ASYMPTOTIC FREEDOM

Dynamics of quarks and gluons described by the Quantum Chromodynamics (QCD)

$$\mathcal{L}_{cl} = \bar{q}_i^{\alpha}\left(i\gamma^{\mu} D_{\mu} - m\right)_{\alpha\beta}^{ij} q_j^{\beta} - \frac{1}{4} F_{\mu\nu}^{a} F_{a}^{\mu\nu}$$

QCD LAGRANGIAN

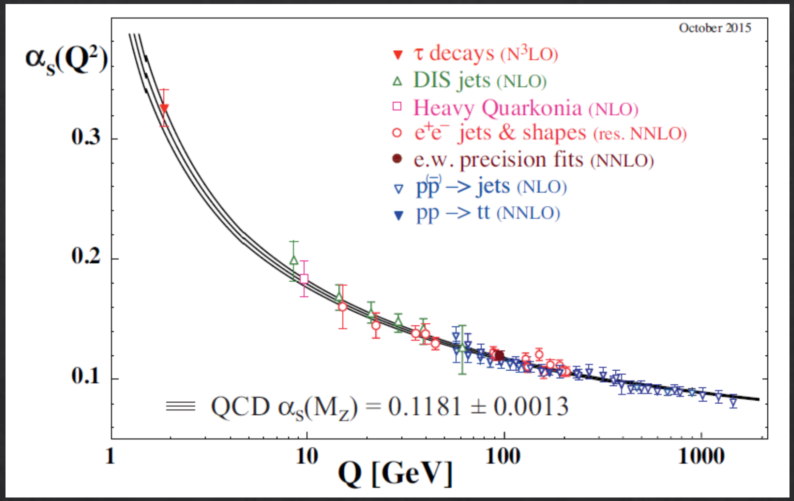

PDG, Chin. Phys. C 38, 010009 (2014-2015)

ASYMPTOTIC FREEDOM

QCD predicts that at very high energy quarks and gluons became weekly interacting

QUARK-GLUON PLASMA (QGP)

Collins and Perry, PRL 34 (1975) 1353

Phenomenological models and lattice QCD indicates the existence of a transition from hadronic matter to QGP at large energy density $\varepsilon \sim 0.5 - 1$ GeV/fm^3

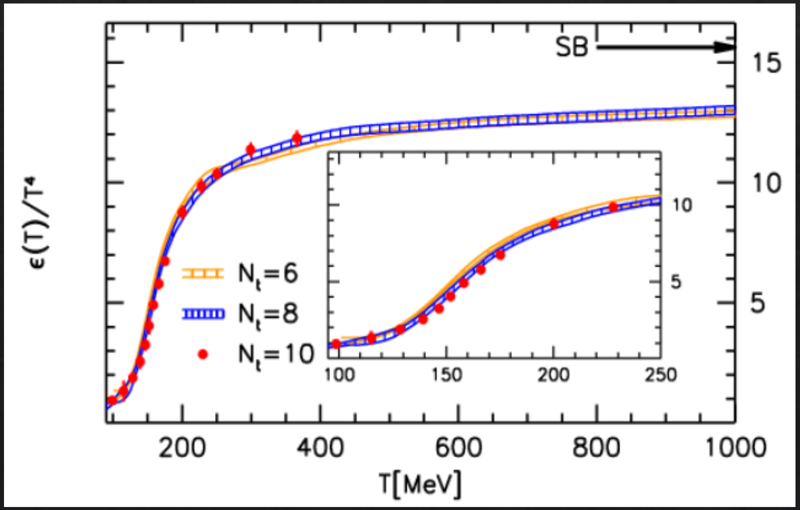

Borsanyi et al., J. High Energ. Phys. 11 (2010) 077

at $\mu = 0$
CROSSOVER
$T_c \approx 155$ MeV

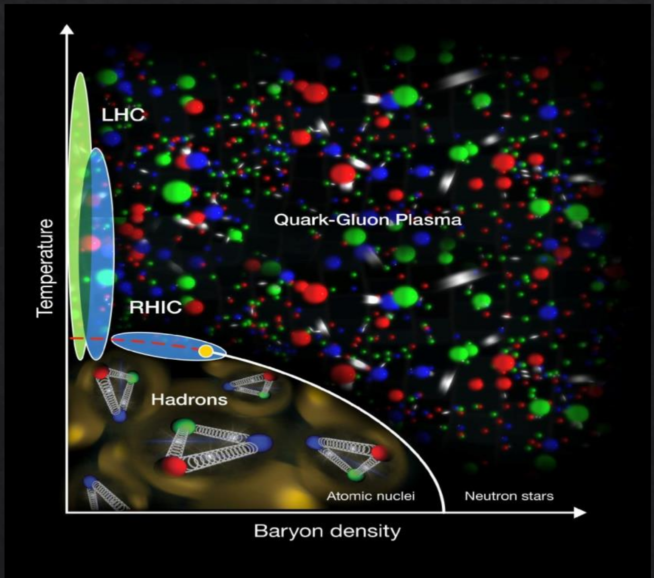

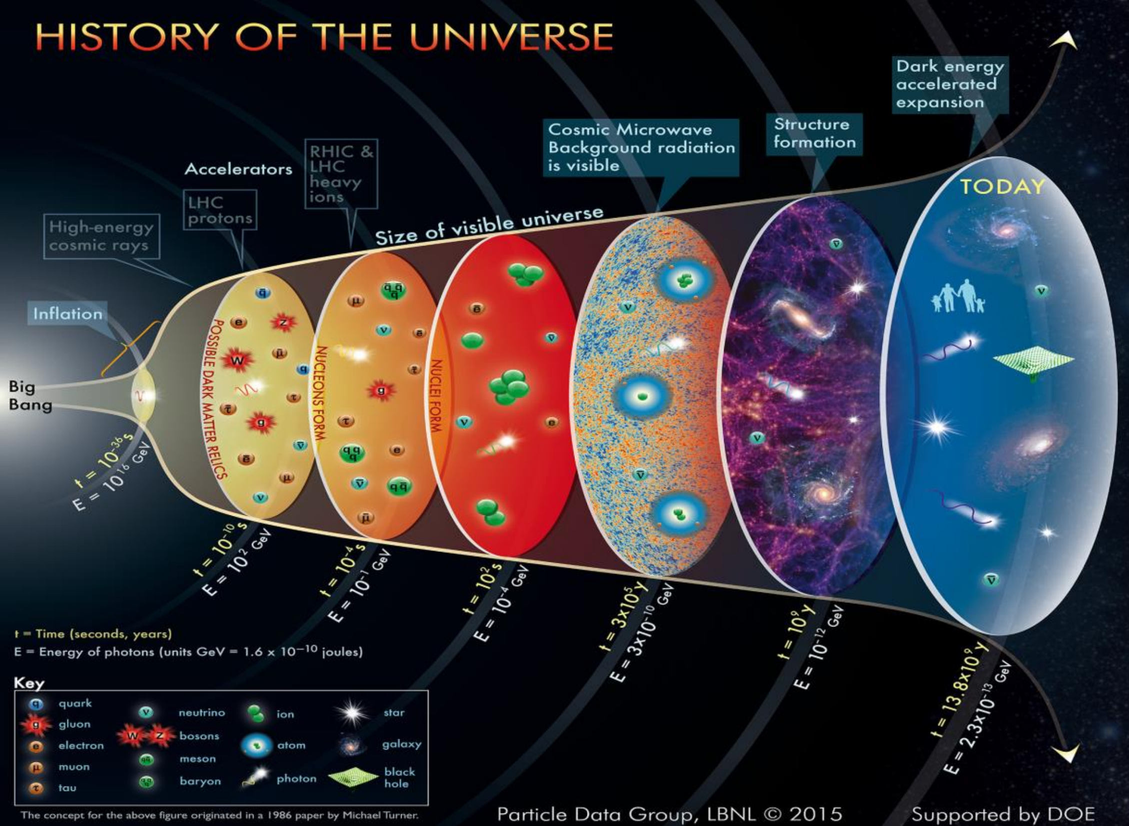

QGP at high temperature and low net baryon density in the

EARLY UNIVERSE

up to ~10 μs after the Big Bang

$T_c \approx 155$ MeV $\approx 2{\cdot}10^{12}$ K

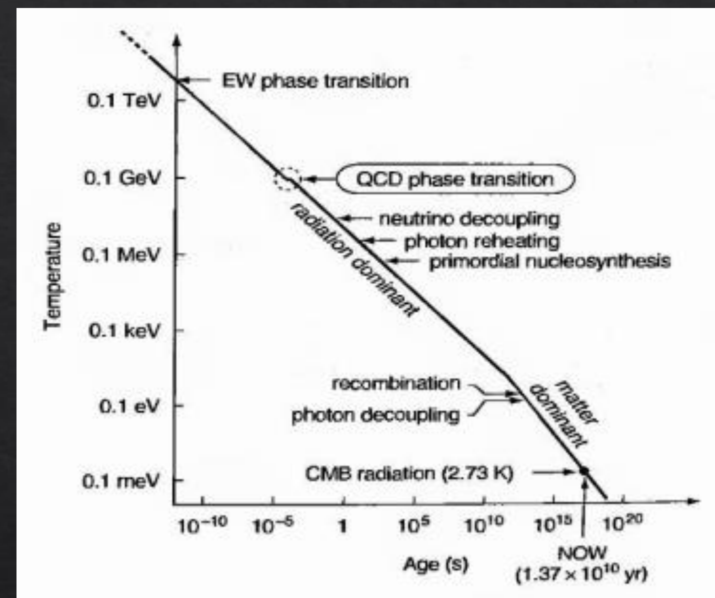

QGP at low temperature and high net baryon density in the core of

NEUTRON STARS

$\rho_c \approx$ 5-10 $\rho_{nm} \approx$ 0.8-1.6 fm$^{-3} \approx 10^{45}$ particles/m^3

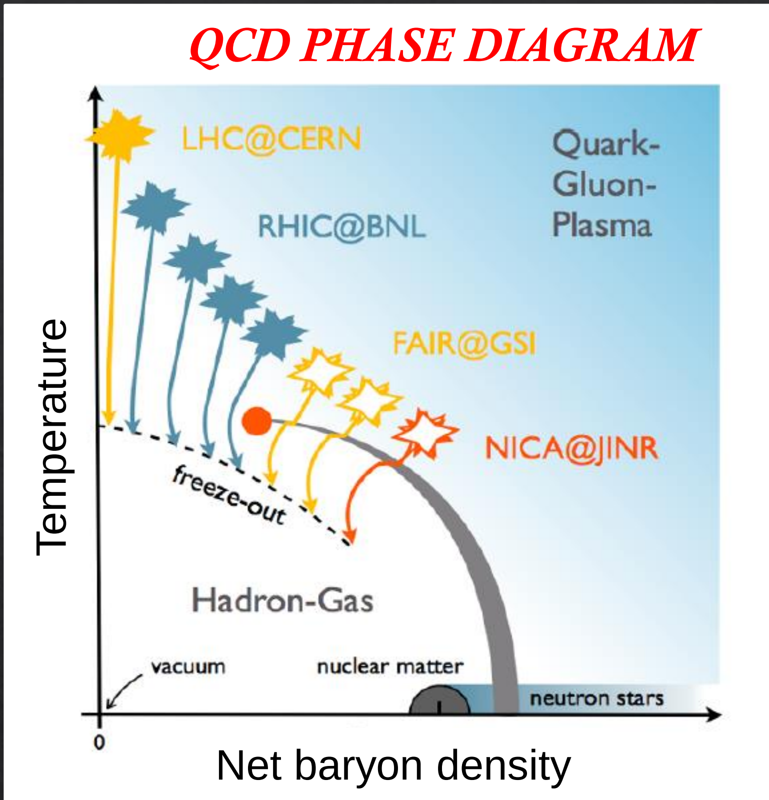

High energy heavy ion collisions

- ✓ allow to experimentally investigate the **QCD PHASE DIAGRAM**
- ✓ recreate the extreme condition of temperature and density required to form the **QUARK-GLUON PLASMA**

Large Hadron Collider (LHC)

Pb+Pb 5.02 *A*TeV

Relativistic Heavy Ion Collider (RHIC)

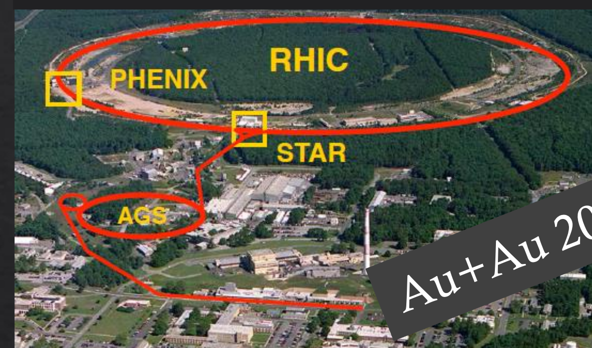

Au+Au 200 *A*GeV

Facility for Antiproton and Ion Research (FAIR)

Au+Au 30 *A*GeV

Au+Au 11 *A*GeV

Nuclotron-based Ion Collider fAcility (NICA)

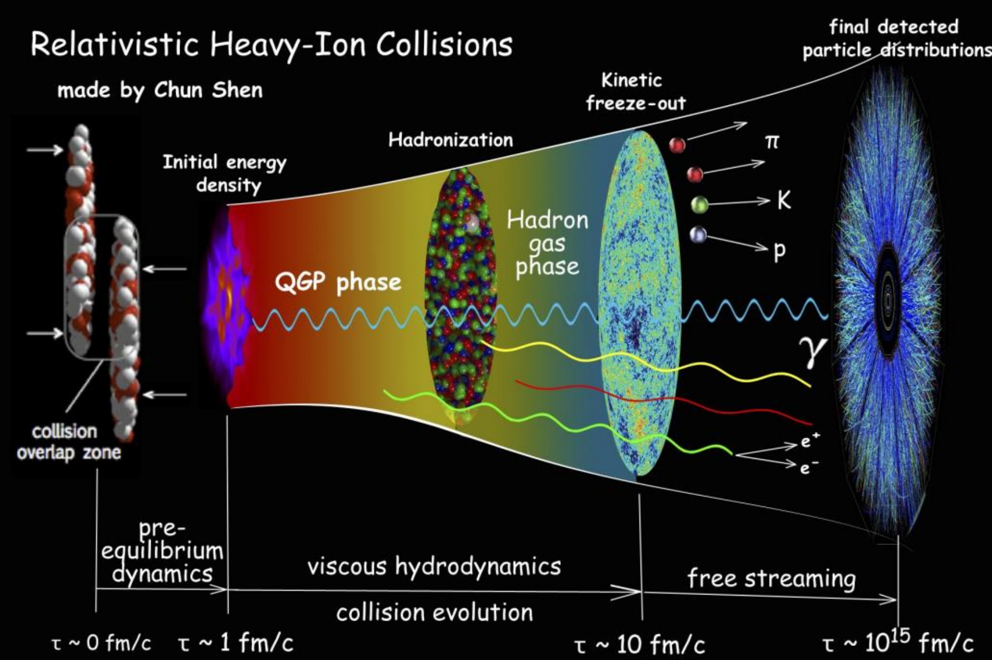

EXPANDING FIREBALL

- $t \sim$ 10-20 fm/c $\sim 10^{-23}$-10^{-22} s
- $x \sim$ 10 fm $\sim 10^{-14}$ m
- $T_{in} \sim$ 300-600 MeV $\sim 10^{12}$ K

Quark-Gluon Plasma

hydrodynamical behaviour with very low η/s and collective flows

$$\frac{dn}{d\phi} \propto 1 + \sum_n 2 v_n(p_T) \cos[n(\phi - \Psi_n)]$$

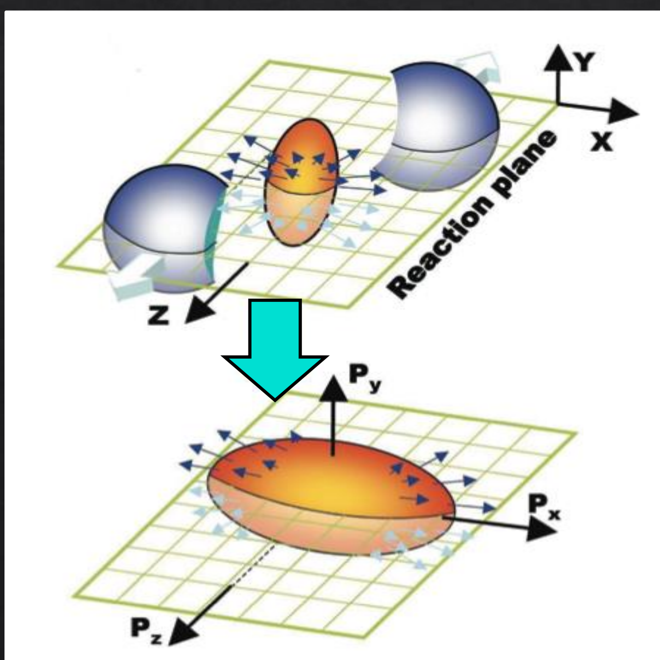

eccentricity

$$\varepsilon = \frac{\langle y^2 - x^2 \rangle}{\langle y^2 + x^2 \rangle}$$

$$v_2 = \left\langle \frac{p_x^2 - p_y^2}{p_x^2 + p_y^2} \right\rangle$$

elliptic flow

$$4\pi\eta/s \approx 1 - 2$$

almost perfect fluid

$\eta/s_{\,qgp} << \eta/s_{\,water} << \eta/s_{\,pitch}$

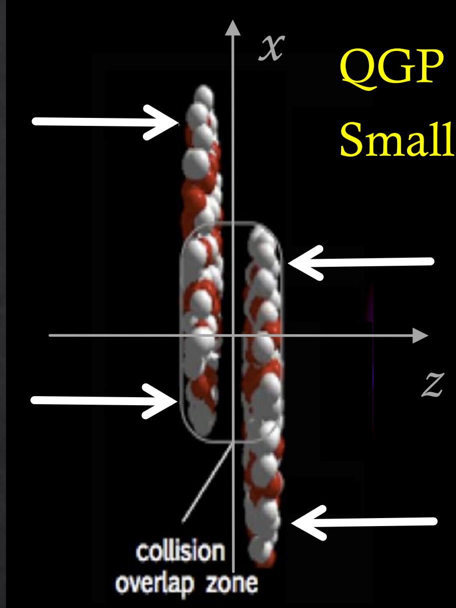

QGP initially expected only in high energy collisions of two heavy ions

Small colliding systems initially regarded as control measurements

Signatures of collective flow found in small systems

p+Pb collisions at LHC, p/d/^{3}He+Au at RHIC

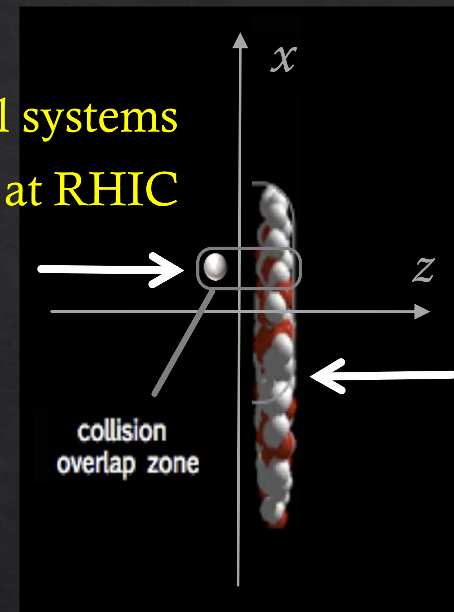

PHENIX Coll., Nature Phys. 15 (2019) 214

nature physics
LETTERS
https://doi.org/10.1038/s41567-018-0360-0

Creation of quark–gluon plasma droplets with three distinct geometries

PHENIX Collaboration*

Experimental studies of the collisions of heavy nuclei at relativistic energies have established the properties of the quark-gluon plasma (QGP), a state of hot, dense nuclear matter in which quarks and gluons are not bound into hadrons[1-4]. In this state, matter behaves as a nearly inviscid fluid[5] that efficiently translates initial spatial anisotropies into correlated momentum anisotropies among the particles produced, creating a common velocity field pattern known as collective flow. In recent years, comparable momentum anisotropies have been measured in small-system proton–proton (p+p) and proton–nucleus (p+A) collisions, despite expectations that the volume and lifetime of the medium produced would be too small to form a QGP. Here we report on the observation of elliptic and triangular flow patterns of charged particles produced in proton–gold (p+Au), deuteron–gold (d+Au) and helium–gold (^{3}He+Au) collisions at a nucleon–nucleon centre-of-mass energy $\sqrt{s_{NN}}$ = 200 GeV. The unique combination of three distinct initial geometries and two flow patterns provides unprecedented model discrimination. Hydrodynamical models, which include the formation of a short-lived QGP droplet, provide the best simultaneous description of these measurements.

COLLECTIVITY IN SMALL SYSTEMS AS SIGN OF QGP DROPLETS?

proton-induced collisions at top RHIC energy

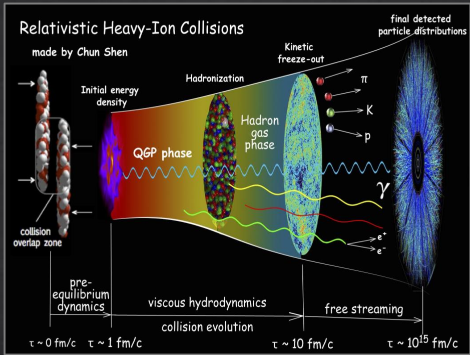

Very intense magnetic fields in the early stage of HICs

HICs

$\sim 10^{18}$-10^{19} G

Many interesting phenomena in HICs driven by the electromagnetic fields (EMF)

CHIRAL MAGNETIC EFFECT

magnetars

$\sim 10^{14}$-10^{15} G

$$J_m = \frac{e^2}{2\pi^2}\mu_5 \boldsymbol{B}$$

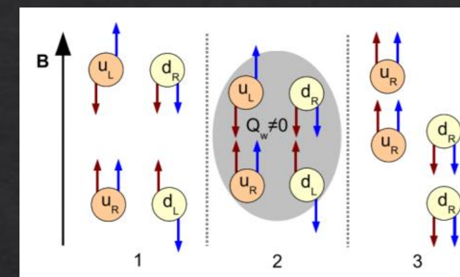

Kharzeev, McLerran and Warringa, NPA 803 (2008) 227

laboratory

$\sim 10^{6}$ G

CHARGE-ODD DIRECTED FLOW

$$v_1^+(y,p_T) \neq v_1^-(y,p_T)$$

$$\boldsymbol{F}_{em} = q(\boldsymbol{E} + \boldsymbol{v}\times\boldsymbol{B})$$

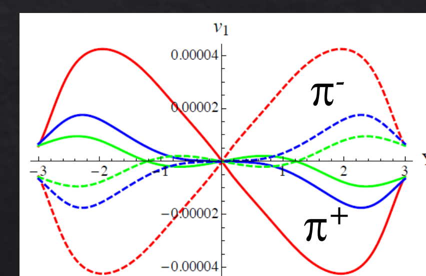

Gursoy, Kharzeev and Rajagopal, PRC 89 (2014) 054905
Voronyuk, Toneev, Voloshin and Cassing, PRC 90 (2014) 064903
Das, Plumari, Greco et al., PLB 768 (2017) 260

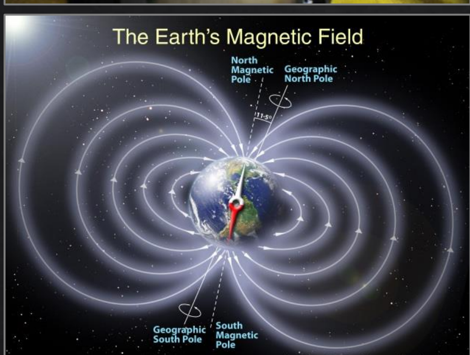

Earth's field

~ 1 G

In p+Au collisions?

PHSD: Parton-Hadron-String Dynamics

non-equilibrium transport approach to describe large and small colliding systems

To study the phase transition from hadronic to partonic matter and QGP properties from a microscopic origin

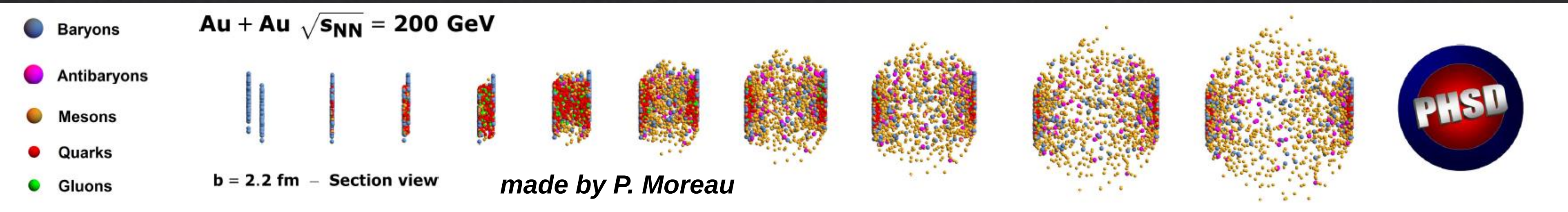

Cassing and Bratkovskaya, PRC 78 (2008) 034919; NPA831 (2009) 215
Cassing, EPJ ST 168 (2009) 3; NPA856 (2011) 162

PHSD: Parton-Hadron-String Dynamics

non-equilibrium transport approach to describe large and small colliding systems

To study the phase transition from hadronic to partonic matter and QGP properties from a microscopic origin

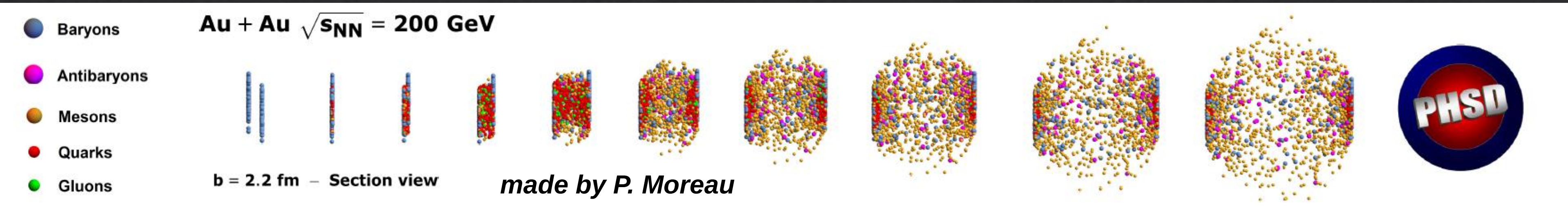

- INITIAL A+A COLLISIONS: nucleon-nucleon collisions lead to the formation of strings that decay to pre-hadrons

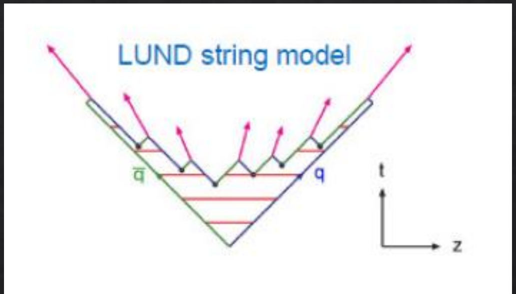

Cassing and Bratkovskaya, PRC 78 (2008) 034919; NPA831 (2009) 215
Cassing, EPJ ST 168 (2009) 3; NPA856 (2011) 162

PHSD: Parton-Hadron-String Dynamics

non-equilibrium transport approach to describe large and small colliding systems

To study the phase transition from hadronic to partonic matter and QGP properties from a microscopic origin

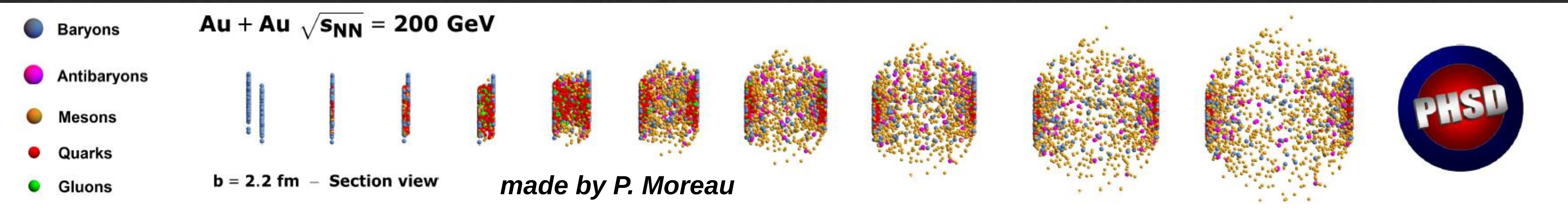

- INITIAL A+A COLLISIONS: nucleon-nucleon collisions lead to the formation of strings that decay to pre-hadrons
- FORMATION OF QGP: if the energy density is above ε_C pre-hadrons dissolve in massive quarks and gluons + mean-field potential

Cassing and Bratkovskaya, PRC 78 (2008) 034919; NPA831 (2009) 215
Cassing, EPJ ST 168 (2009) 3; NPA856 (2011) 162

PHSD: Parton-Hadron-String Dynamics

non-equilibrium transport approach to describe large and small colliding systems

To study the phase transition from hadronic to partonic matter and QGP properties from a microscopic origin

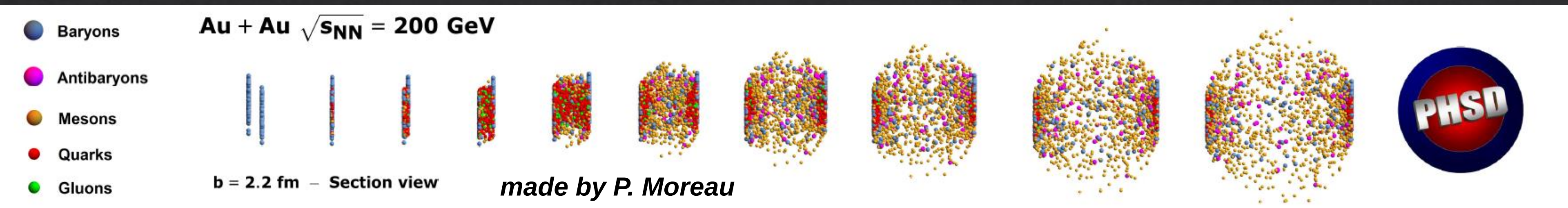

- INITIAL A+A COLLISIONS: nucleon-nucleon collisions lead to the formation of strings that decay to pre-hadrons
- FORMATION OF QGP: if the energy density is above ε_C pre-hadrons dissolve in massive quarks and gluons + mean-field potential
- PARTONIC STAGE: evolution based on Generalized Transport Equations with parton properties defined by the Dynamical Quasi-Particle Model

Cassing and Bratkovskaya, PRC 78 (2008) 034919; NPA831 (2009) 215
Cassing, EPJ ST 168 (2009) 3; NPA856 (2011) 162

PHSD: Parton-Hadron-String Dynamics

non-equilibrium transport approach to describe large and small colliding systems

To study the phase transition from hadronic to partonic matter and QGP properties from a microscopic origin

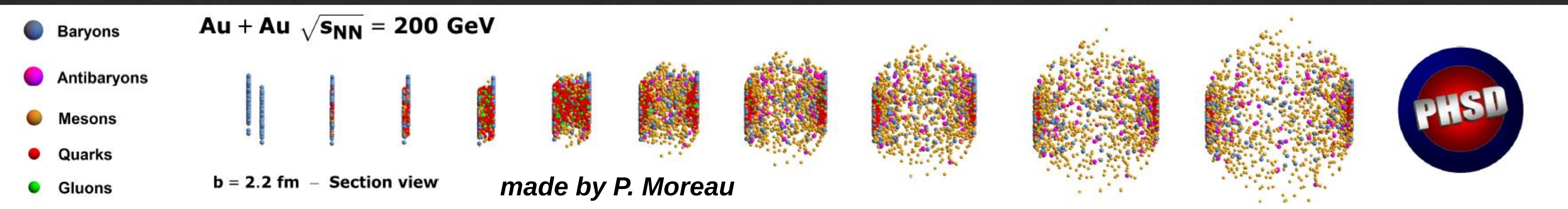

- INITIAL A+A COLLISIONS: nucleon-nucleon collisions lead to the formation of strings that decay to pre-hadrons
- FORMATION OF QGP: if the energy density is above ε_C pre-hadrons dissolve in massive quarks and gluons + mean-field potential
- PARTONIC STAGE: evolution based on Generalized Transport Equations with parton properties defined by the Dynamical Quasi-Particle Model
- HADRONIZATION: massive off-shell partons with broad spectral functions hadronize to off-shell baryon and mesons

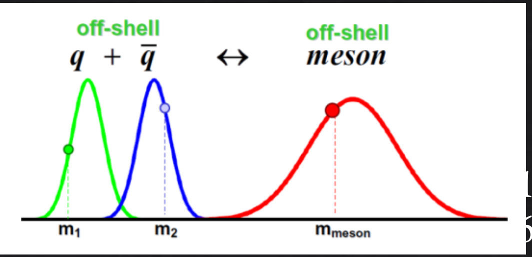

Cassing and Bratkovskaya ... 1 (2009) 215
Cassin... 5 (2011) 162

PHSD: Parton-Hadron-String Dynamics

non-equilibrium transport approach to describe large and small colliding systems

To study the phase transition from hadronic to partonic matter and QGP properties from a microscopic origin

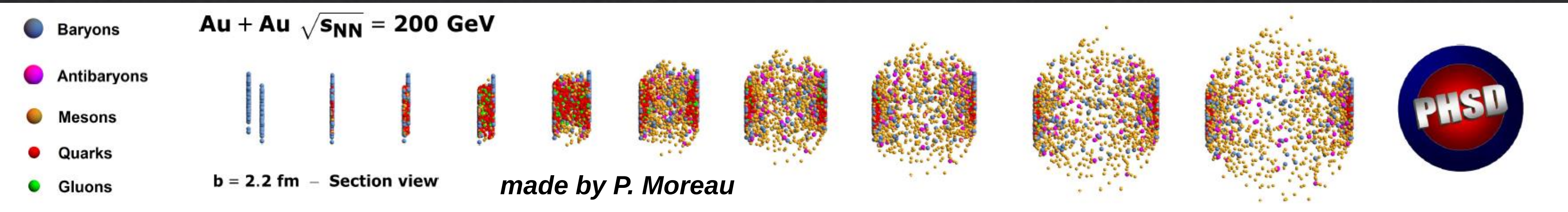

- INITIAL A+A COLLISIONS: nucleon-nucleon collisions lead to the formation of strings that decay to pre-hadrons
- FORMATION OF QGP: if the energy density is above ε_C pre-hadrons dissolve in massive quarks and gluons + mean-field potential
- PARTONIC STAGE: evolution based on Generalized Transport Equations with parton properties defined by the Dynamical Quasi-Particle Model
- HADRONIZATION: massive off-shell partons with broad spectral functions hadronize to off-shell baryon and mesons
- HADRONIC PHASE: evolution based on Generalized Transport Equations with hadron-hadron interactions

Cassing and Bratkovskaya, PRC 78 (2008) 034919; NPA831 (2009) 215
Cassing, EPJ ST 168 (2009) 3; NPA856 (2011) 162

PHSD: Parton-Hadron-String Dynamics

non-equilibrium transport approach to describe large and small colliding systems

To study the phase transition from hadronic to partonic matter and QGP properties from a microscopic origin

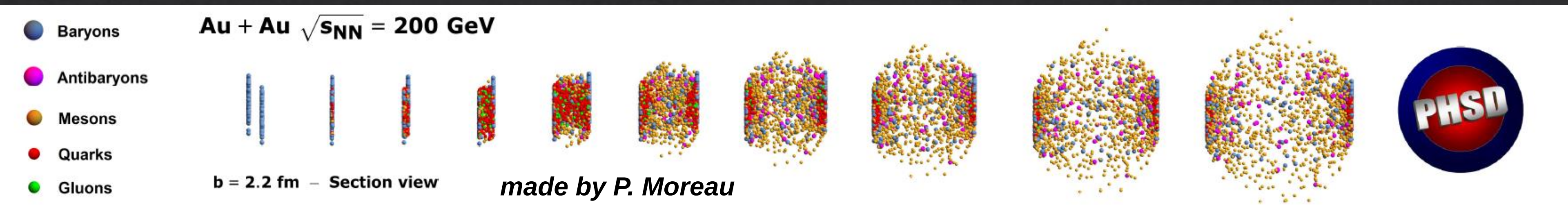

- INITIAL A+A COLLISIONS
- FORMATION OF QGP
- PARTONIC STAGE
- HADRONIZATION
- HADRONIC PHASE

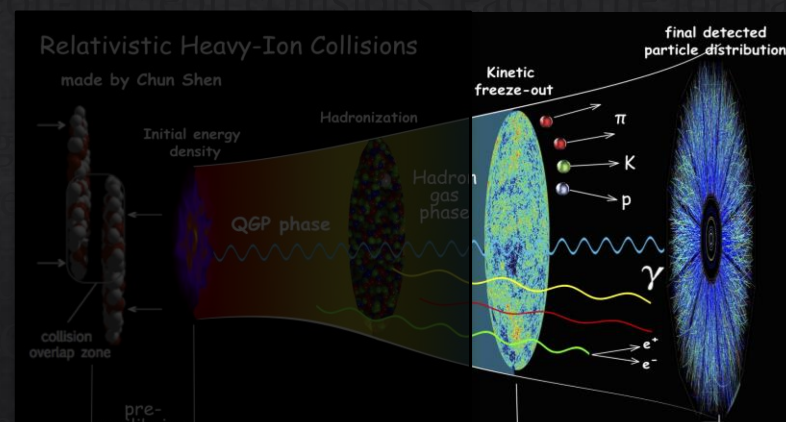

good description of A–A collisions
from the lower SPS to the top LHC energies
for bulk and electromagnetic observables

Generalized Transport Equations (GTE)

After the first order gradient expansion of the Wigner transformed Kadanoff-Baym equations and separation into the real and imaginary parts one obtain GTE which describes the dynamics of broad strongly interacting quantum states

drift term | Vlasov term | backflow term | collision term = ‚gain‘ - ‚loss‘ term

$$\diamond \{ P^2 - M_0^2 - Re\Sigma^{ret}_{XP} \} \{ S^{<}_{XP} \} - \diamond \{ \Sigma^{<}_{XP} \} \{ Re S^{ret}_{XP} \} = \frac{i}{2} [\Sigma^{>}_{XP} S^{<}_{XP} - \Sigma^{<}_{XP} S^{>}_{XP}]$$

$$\diamond \{ F_1 \} \{ F_2 \} := \frac{1}{2} \left(\frac{\partial F_1}{\partial X_\mu} \frac{\partial F_2}{\partial P^\mu} - \frac{\partial F_1}{\partial P_\mu} \frac{\partial F_2}{\partial X^\mu} \right)$$

off-shell behavior

GTE govern the propagation of the Green functions $i\, S^{<}_{XP} = A_{XP}\, N_{XP}$

particle spectral function (A_{XP}); number of particles (N_{XP})

Dressed propagators (S_q, Δ_g)

$$S = (P^2 - \Sigma^2)^{-1}$$

with complex self-energies (Σ_q, Π_g):

$$\Sigma = m^2 - i2\gamma\omega$$

- ❖ the real part describes a dynamically generated mass (m_q, m_g)
- ❖ the imaginary part describes the interaction width (γ_q, γ_g)

Cassing and Juchem, NPA 665 (2000) 377; 672 (2000) 417; 677 (2000) 445

Dynamical QuasiParticel Model (DQPM)

The DQPM describes QGP in terms of interacting quasiparticle: massive quarks and gluons with Lorentzian spectral functions

$$A_j(\omega,\mathbf{p}) = \frac{\gamma_j}{\tilde{E}_j}\left(\frac{1}{(\omega-\tilde{E}_j)^2+\gamma_j^2} - \frac{1}{(\omega+\tilde{E}_j)^2+\gamma_j^2}\right)$$

$$\tilde{E}_j = p^2 + m^2 - \gamma^{\,2}$$

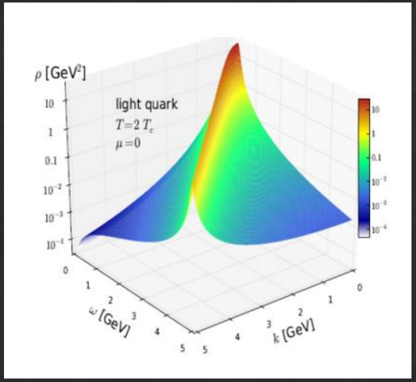

GLUONS QUARKS

MASSES

$$m_g^2 = \frac{g^2}{6}\left(N_c + \frac{1}{2}N_f\right)T^2, \qquad m_q^2 = g^2\frac{N_c^2-1}{8N_c}T^2$$

WIDTHS

$$\gamma_g = \frac{1}{3}N_c\frac{g^2T}{8\pi}\ln\left(\frac{2c}{g^2}+1\right), \quad \gamma_q = \frac{1}{3}\frac{N_c^2-1}{2N_c}\frac{g^2T}{8\pi}\ln\left(\frac{2c}{g^2}+1\right)$$

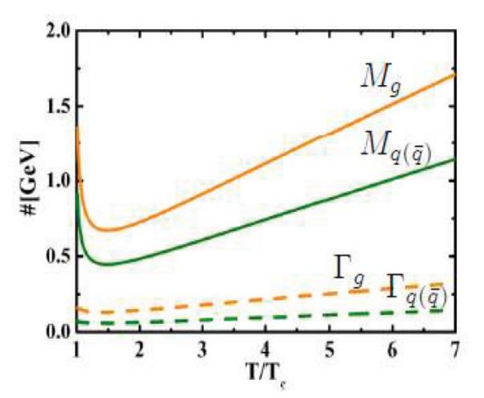

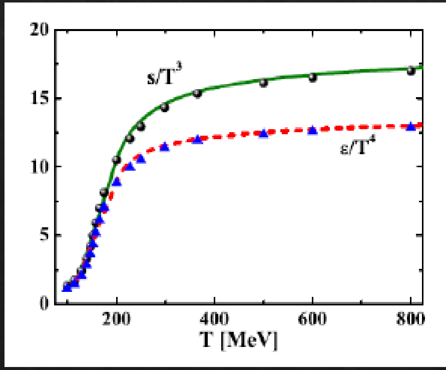

$$g^2(T/T_c) = \frac{48\pi^2}{(11N_c - 2N_f)\ln(\lambda^2(T/T_c - T_s/T_c)^2}$$

RUNNING COUPLING

parameters from fit of lattice QCD thermodinamics

Peshier, PRD 70 (2004) 034016
Peshier and Cassing, PRL 94 (2005) 172301
Cassing, NPA 791 (2007) 365; NPA 793 (2007)

PHSD extended to include chemical potential dependence of scattering cross section

Moreau, Soloveva, LO, Song, Cassing and Bratkovskaya, PRC 100 (2019) 014911

PHSD + electromagnetic fields

PHSD has been extended including the dynamical formation and evolution of the retarded electomagnetic field (EMF) and its influence on the quasi-particle (QP) dynamics

Voronyuk *et al.*, PRC 83 (2011) 054911
Toneev *et al.*, PRC 85 (2012) 034910; PRC 86 (2012) 064907; PRC 95 (2017) 034911

TRANSPORT EQUATION

$$\left\{ \frac{\partial}{\partial t} + \left(\frac{\mathbf{p}}{p_0} + \nabla_{\mathbf{p}} U \right) \nabla_{\mathbf{r}} + (-\nabla_{\mathbf{r}} U + e\mathbf{E} + e\mathbf{v} \times \mathbf{B}) \nabla_{\mathbf{p}} \right\} f = C_{\mathrm{coll}}(f, f_1, \ldots, f_N)$$

Lorentz force

MAXWELL EQUATIONS

$$\nabla \cdot \mathbf{B} = 0 \qquad \nabla \times \mathbf{E} = -\frac{\partial \mathbf{B}}{\partial t} \qquad \nabla \cdot \mathbf{E} = 4\pi\rho \qquad \nabla \times \mathbf{B} = \frac{\partial \mathbf{E}}{\partial t} + \frac{4\pi}{c}\mathbf{j}$$

charge distribution **electric current**

consistent solution of particle and field evolution equations

retarded electromagnetic fields

$$\mathbf{B} = \nabla \times \mathbf{A}, \qquad \mathbf{E} = -\nabla\Phi - \frac{\partial \mathbf{A}}{\partial t}$$

General solution of the wave equation for the electromagnetic potentials

$$\mathbf{A}(\mathbf{r},t) = \frac{1}{4\pi}\int \frac{\mathbf{j}(\mathbf{r}',t')\ \delta(t-t'-|\mathbf{r}-\mathbf{r}'|/c)}{|\mathbf{r}-\mathbf{r}'|}\ d^3r'dt'$$

$$\Phi(\mathbf{r},t) = \frac{1}{4\pi}\int \frac{\rho(\mathbf{r}',t')\ \delta(t-t'-|\mathbf{r}-\mathbf{r}'|/c)}{|\mathbf{r}-\mathbf{r}'|}\ d^3r'dt'$$

$$\mathbf{r}' \equiv \mathbf{r}(t')$$

$$t' = t - \frac{\mathbf{r}-\mathbf{r}'}{c}$$

Liénard-Wiechert potentials for a moving point-like charge

$$\Phi(\mathbf{r},t) = \frac{e}{4\pi}\left[\frac{1}{R(1-\mathbf{n}\cdot\boldsymbol{\beta})}\right]_{\mathrm{ret}} \qquad \mathbf{A}(\mathbf{r},t) = \frac{e}{4\pi}\left[\frac{\boldsymbol{\beta}}{R(1-\mathbf{n}\cdot\boldsymbol{\beta})}\right]_{\mathrm{ret}}$$

ret: evaluated at the times t'

$$\mathbf{R} = \mathbf{r} - \mathbf{r}'$$

$$\mathbf{n} = \frac{\mathbf{R}}{R}$$

$$\boldsymbol{\beta} = \frac{\mathbf{v}}{c}$$

retarded electromagnetic fields

Retarded electric and magnetic fields for a moving point-like charge

$$\mathbf{E}(\mathbf{r},t) = \frac{e}{4\pi}\left[\frac{\mathbf{n}-\boldsymbol{\beta}}{(1-\mathbf{n}\cdot\boldsymbol{\beta})^3\gamma^2R^2} + \frac{\mathbf{n}\times\left((\mathbf{n}-\boldsymbol{\beta})\times\dot{\boldsymbol{\beta}}\right)}{(1-\mathbf{n}\cdot\boldsymbol{\beta})^3 cR}\right]_{\mathrm{ret}} \qquad \mathbf{B}(\mathbf{r},t) = [\mathbf{n}\times\mathbf{E}(\mathbf{r},t)]_{\mathrm{ret}}$$

elastic Coulomb scatterings

inelastic bremsstrahlung processes

$$\mathbf{R} = \mathbf{r}-\mathbf{r}' \qquad \mathbf{n} = \frac{\mathbf{R}}{R} \qquad \boldsymbol{\beta} = \frac{\mathbf{v}}{c}$$

Neglecting the acceleration

$$e\mathbf{E}(t,\mathbf{r}) = \alpha_{em}\frac{1-\beta^2}{\left[(\mathbf{R}\cdot\boldsymbol{\beta})^2 + R^2(1-\beta^2)\right]^{3/2}}\mathbf{R}$$

$$e\mathbf{B}(t,\mathbf{r}) = \alpha_{em}\frac{1-\beta^2}{\left[(\mathbf{R}\cdot\boldsymbol{\beta})^2 + R^2(1-\beta^2)\right]^{3/2}}\boldsymbol{\beta}\times\mathbf{R}$$

magnetic field created by a single freely moving charge

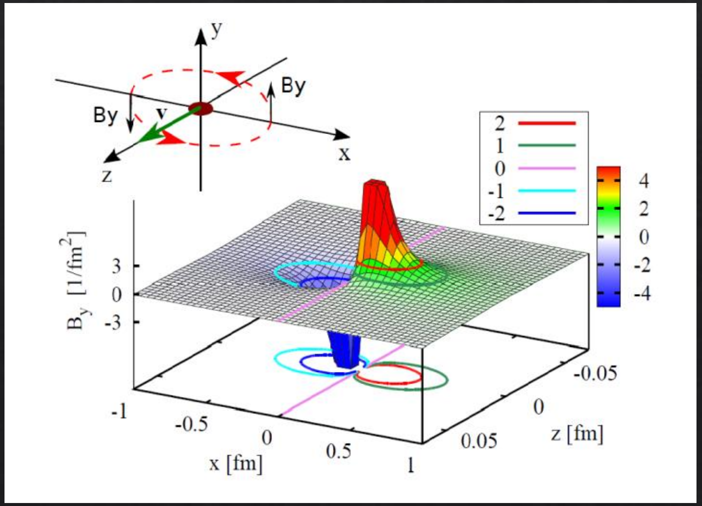

Voronyuk *et al*. (HSD), PRC 83 (2011) 054911

electromagnetic fields in HICs

in a nuclear collision the magnetic field is a superposition of solenoidal fields from different moving charges

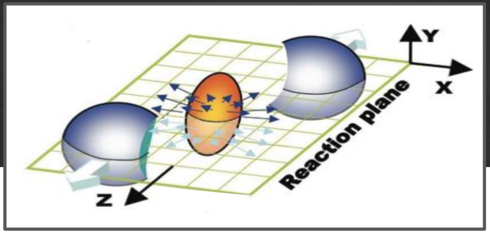

Au+Au @RHIC 200 GeV – b = 10 fm

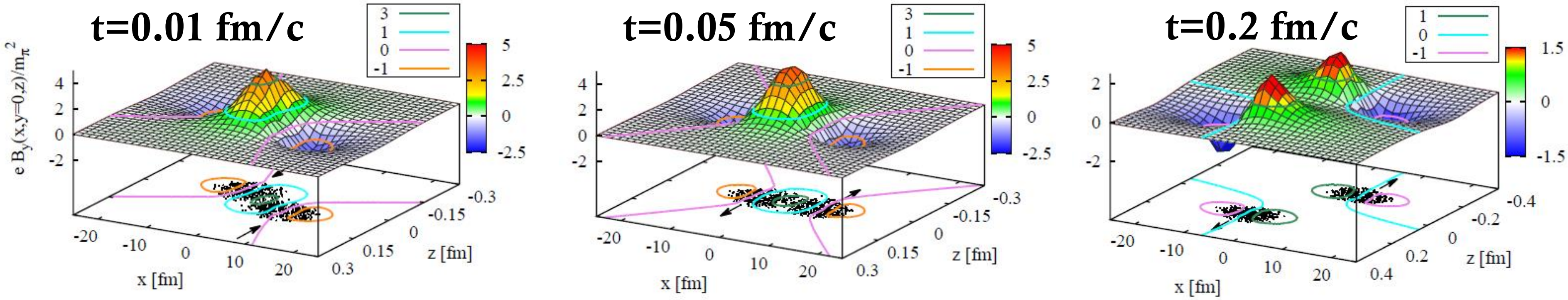

Voronyuk *et al*. (HSD), PRC 83 (2011) 054911

electromagnetic fields in HICs

in a nuclear collision the magnetic field is a superposition of solenoidal fields from different moving charges

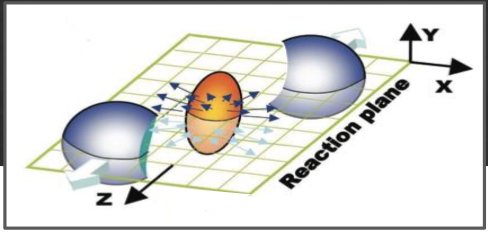

Au+Au @RHIC 200 GeV – b = 10 fm

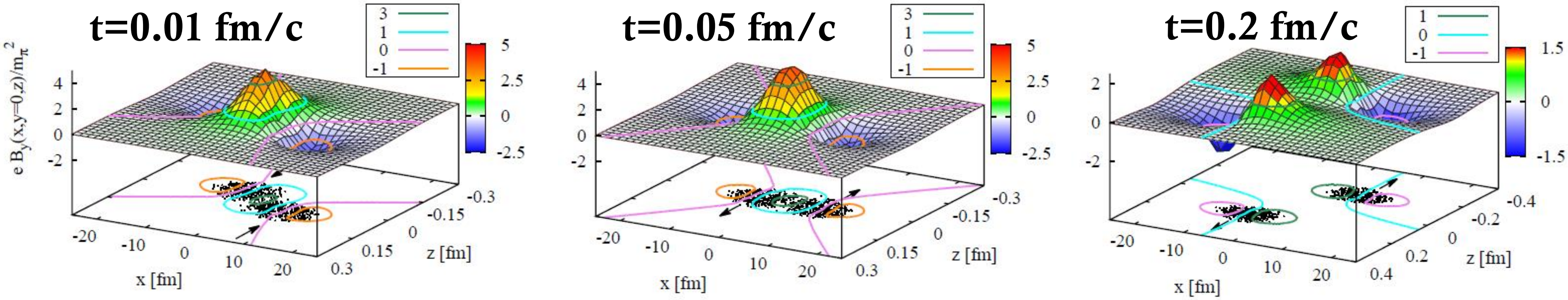

MAGNETIC FIELD

- ❖ dominated by the y-component
- ❖ maximal strength reached during nuclear overlapping time
- ❖ only due to spectators up to $t \sim 1$ fm/c
- ❖ drops down by three orders of magnitude and become comparable with that from participants

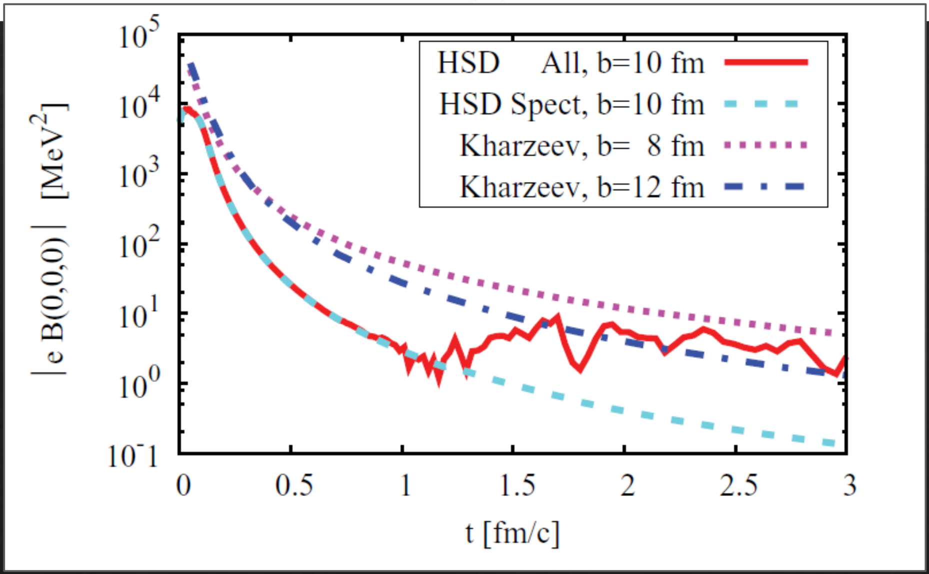

Voronyuk *et al*. (HSD), PRC 83 (2011) 054911

electromagnetic fields in HICs

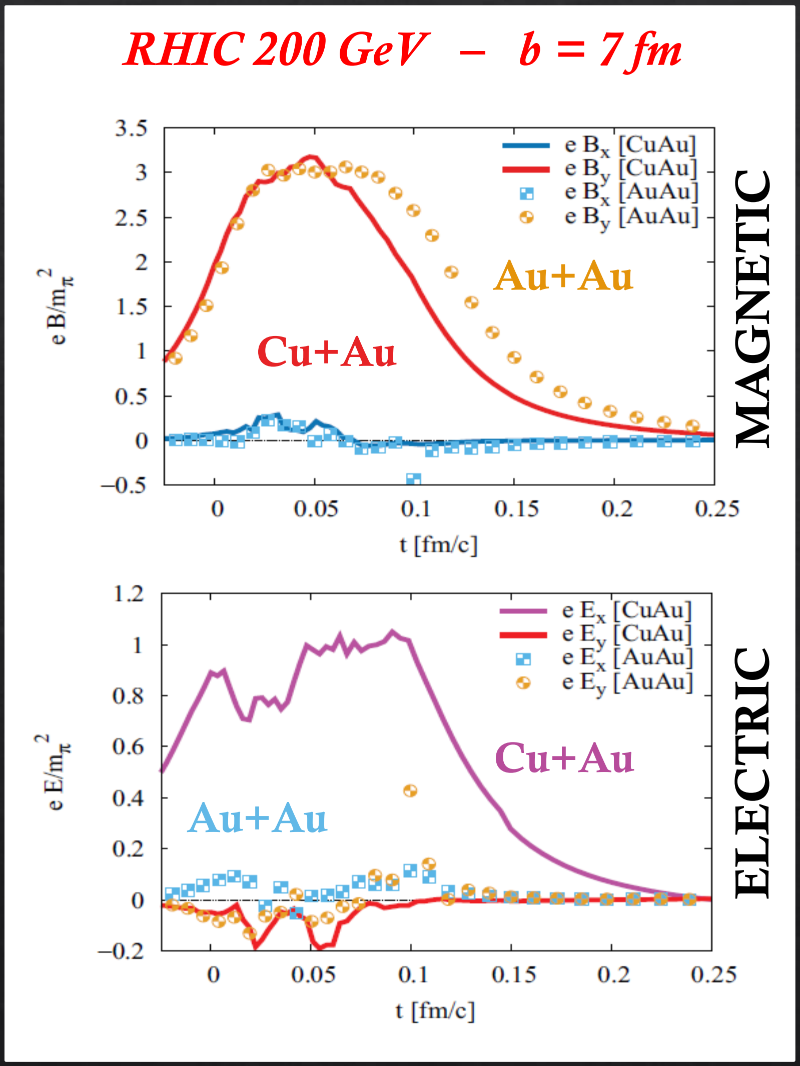

Voronyuk *et al*. (PHSD), PRC 90 (2014) 064903
Toneev *et al*. (PHSD), PRC 95 (2017) 034911

✓ SYMMETRIC SYSTEMS (e.g. Au+Au)
transverse momentum increments due to electric and magnetic fields compensate each other

✓ ASYMMETRIC SYSTEMS (e.g. Cu+Au)
an intense electric fields directed from the heavy nuclei to light one appears in the overlap region

electromagnetic fields in HICs

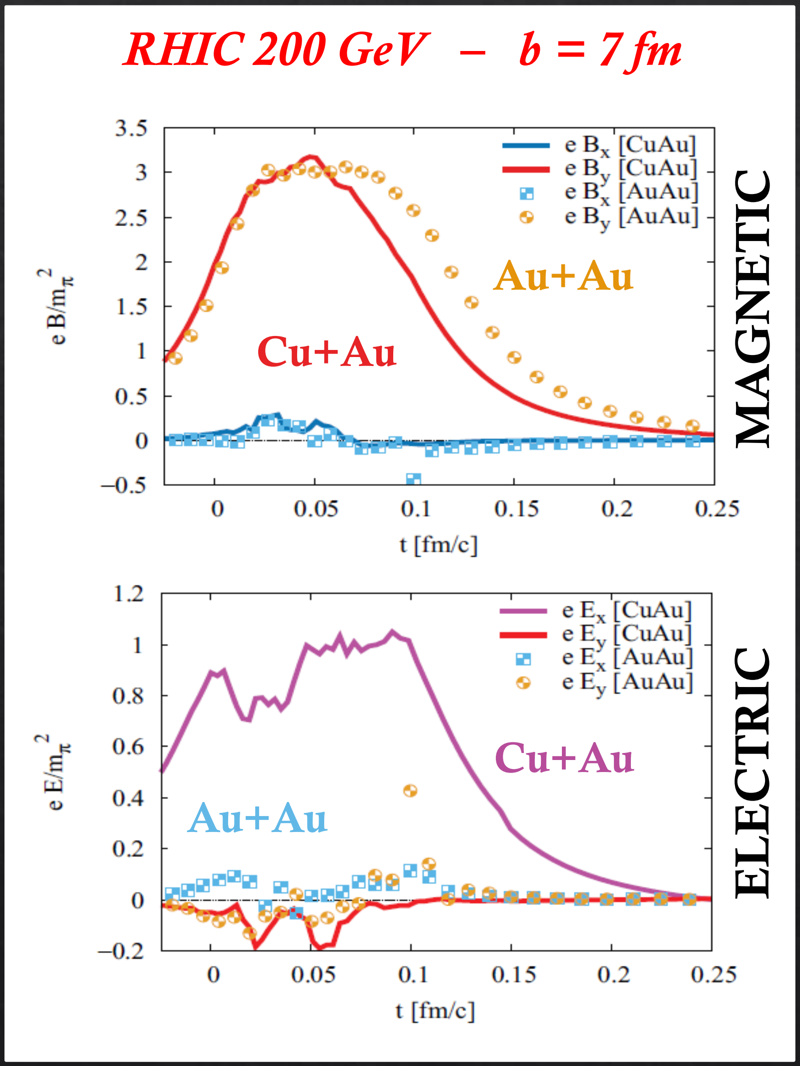

Voronyuk *et al*. (PHSD), PRC 90 (2014) 064903
Toneev *et al*. (PHSD), PRC 95 (2017) 034911

✓ SYMMETRIC SYSTEMS (e.g. Au+Au)
transverse momentum increments due to electric and magnetic fields compensate each other

✓ ASYMMETRIC SYSTEMS (e.g. Cu+Au)
an intense electric fields directed from the heavy nuclei to light one appears in the overlap region

SMALL SYSTEMS (e.g. p+Au)?

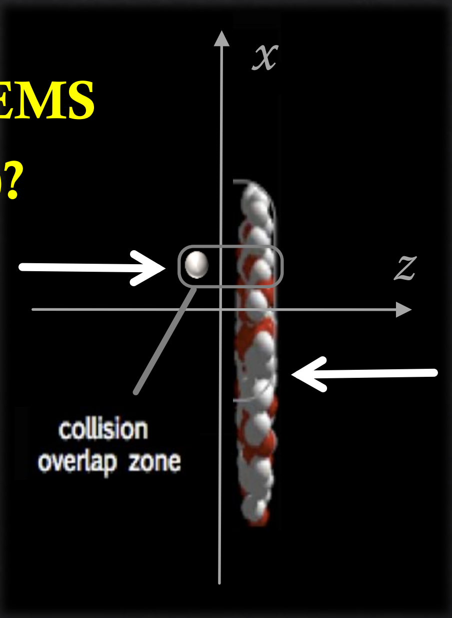

p+Au: electromagnetic fields

Au+Au @ RHIC 200 GeV b=7 fm

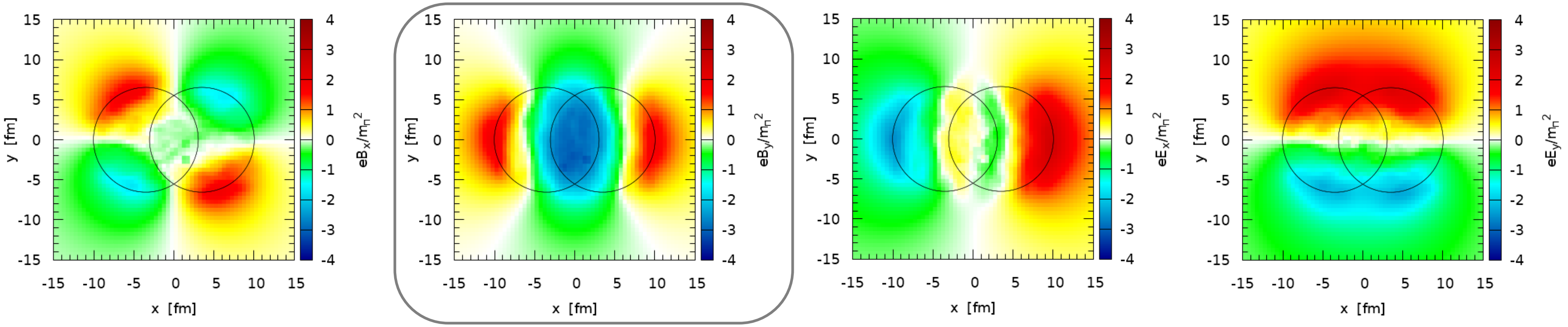

B_x B_y E_x E_y

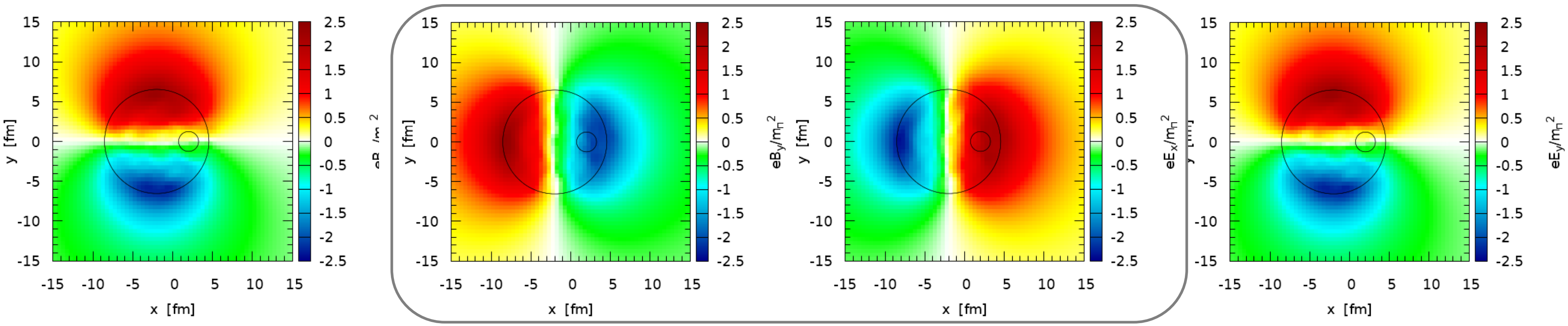

p+Au @ RHIC 200 GeV b=4 fm

LO, Moreau, Voronyuk and Bratkovskaya, 1909.06770

p+Au: electromagnetic fields

p+Au @ RHIC 200 GeV b=4 fm

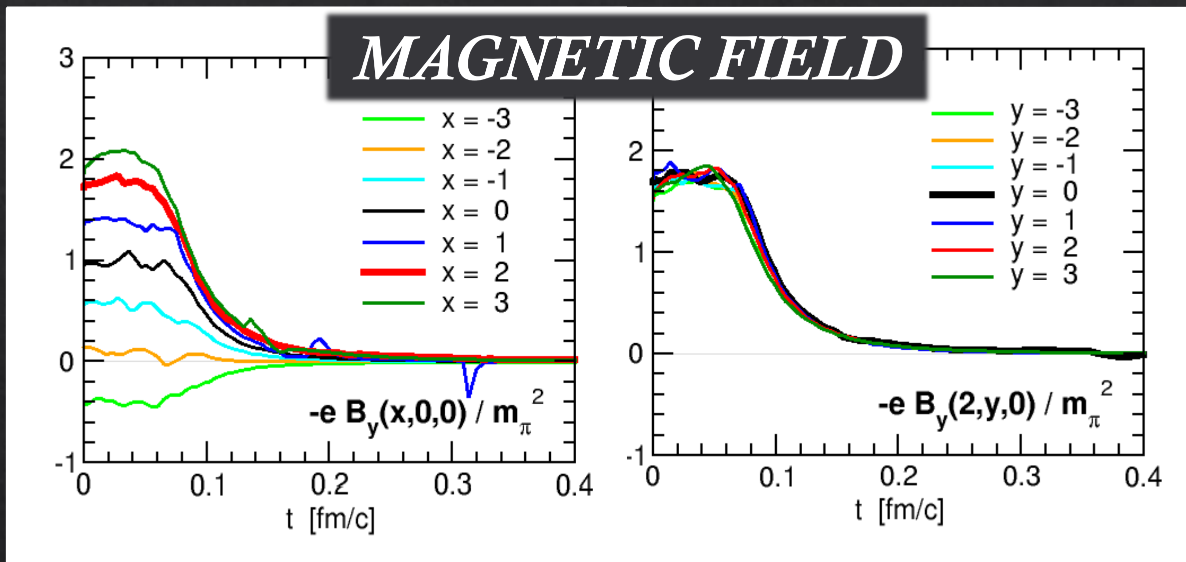

B_y

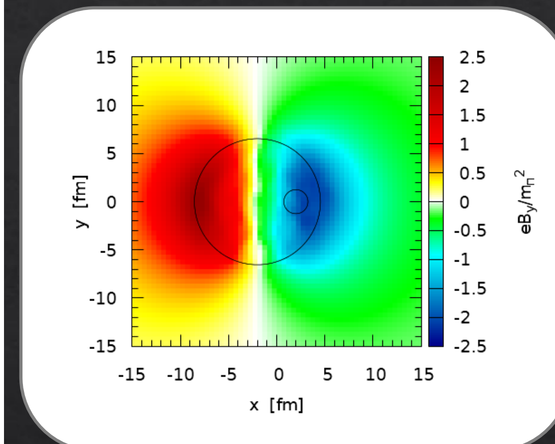

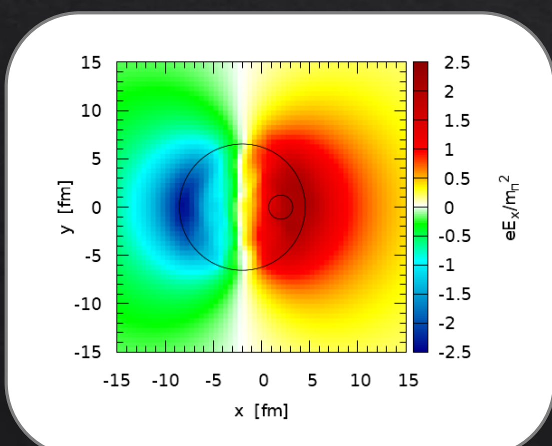

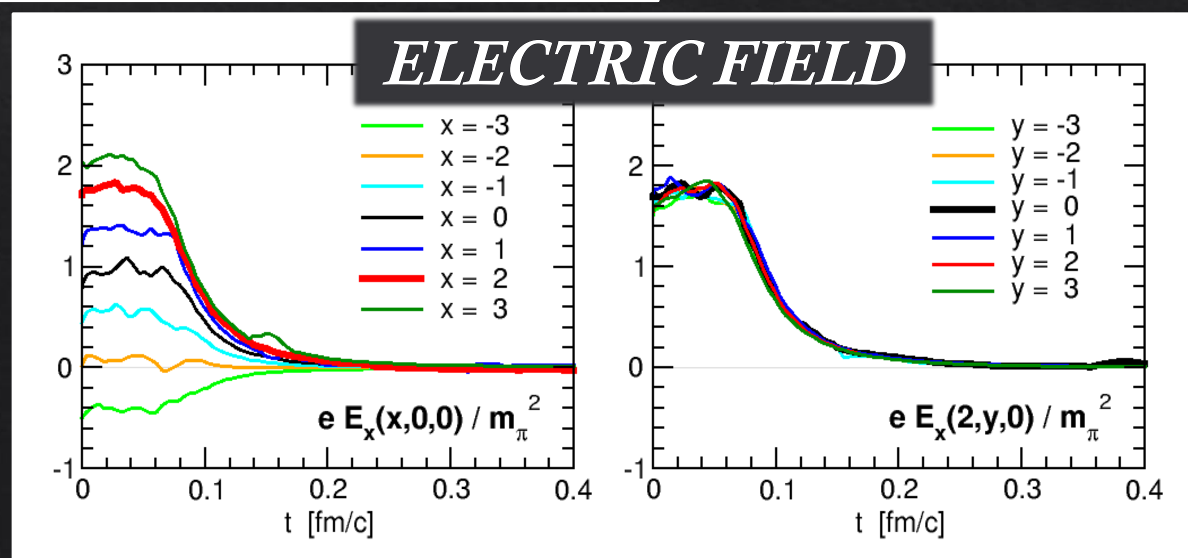

E_x

centrality in small systems

In heavy ion collisions centrality characterizes the amount of overlap or size of the fireball in the collision region

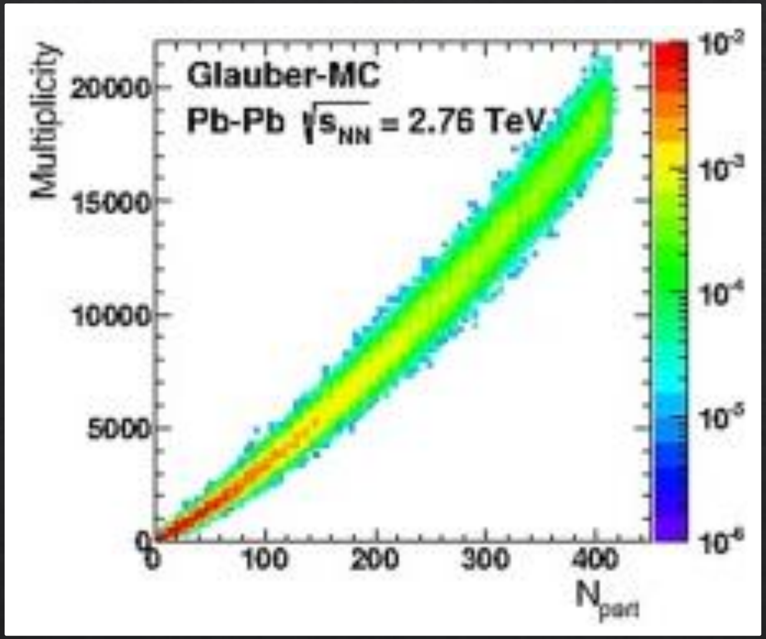

ALICE, NPA 932 (2014) 399

Correlation between participant number and charged particle multiplicity at midrapidity

p+Au: centrality determination

In heavy ion collisions centrality characterizes the amount of overlap or size of the fireball in the collision region

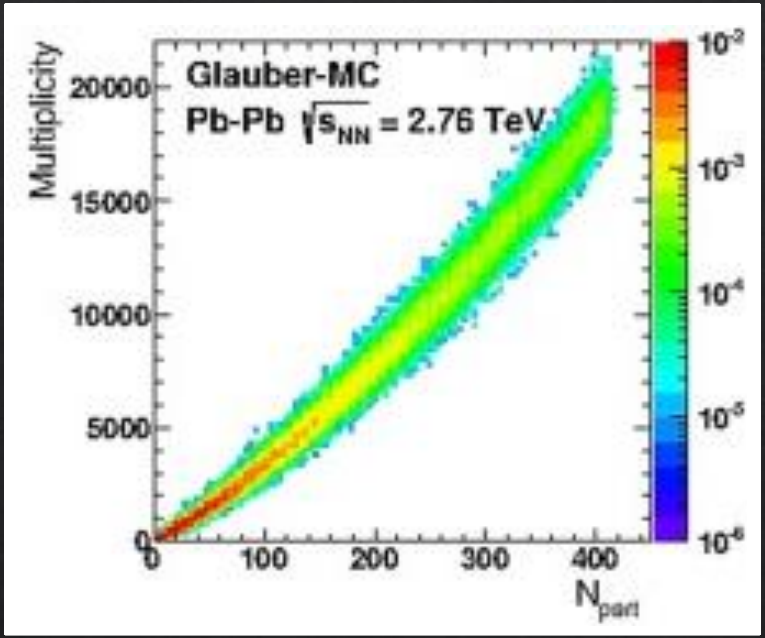

ALICE, NPA 932 (2014) 399

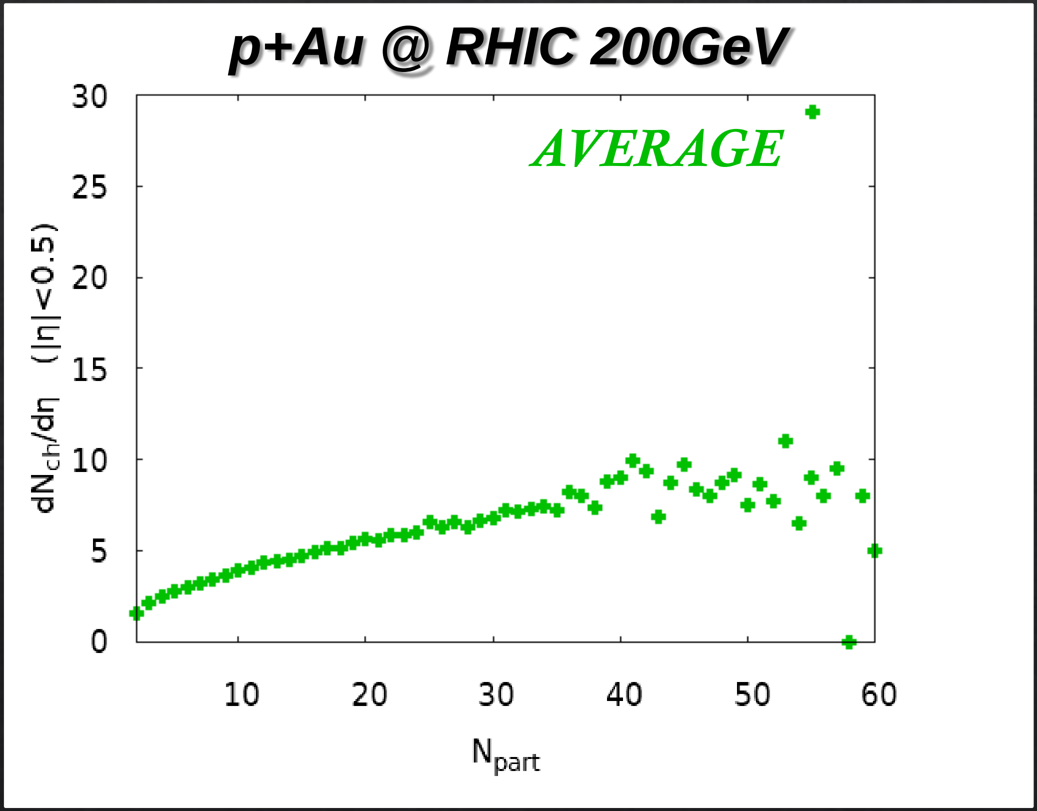

Correlation between participant number and charged particle multiplicity at midrapidity

p+Au: centrality determination

In heavy ion collisions centrality characterizes the amount of overlap or size of the fireball in the collision region

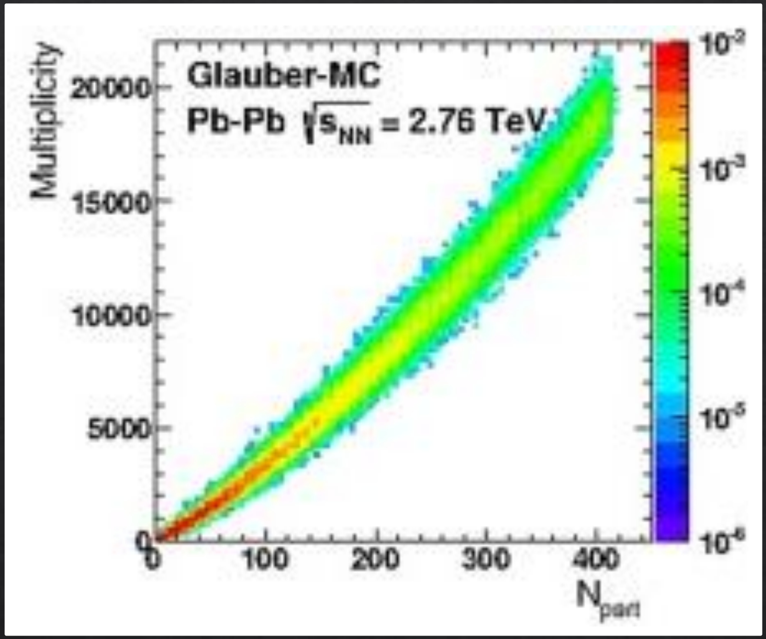

ALICE, NPA 932 (2014) 399

LO, Moreau, Voronyuk and Bratkovskaya, 1909.06770

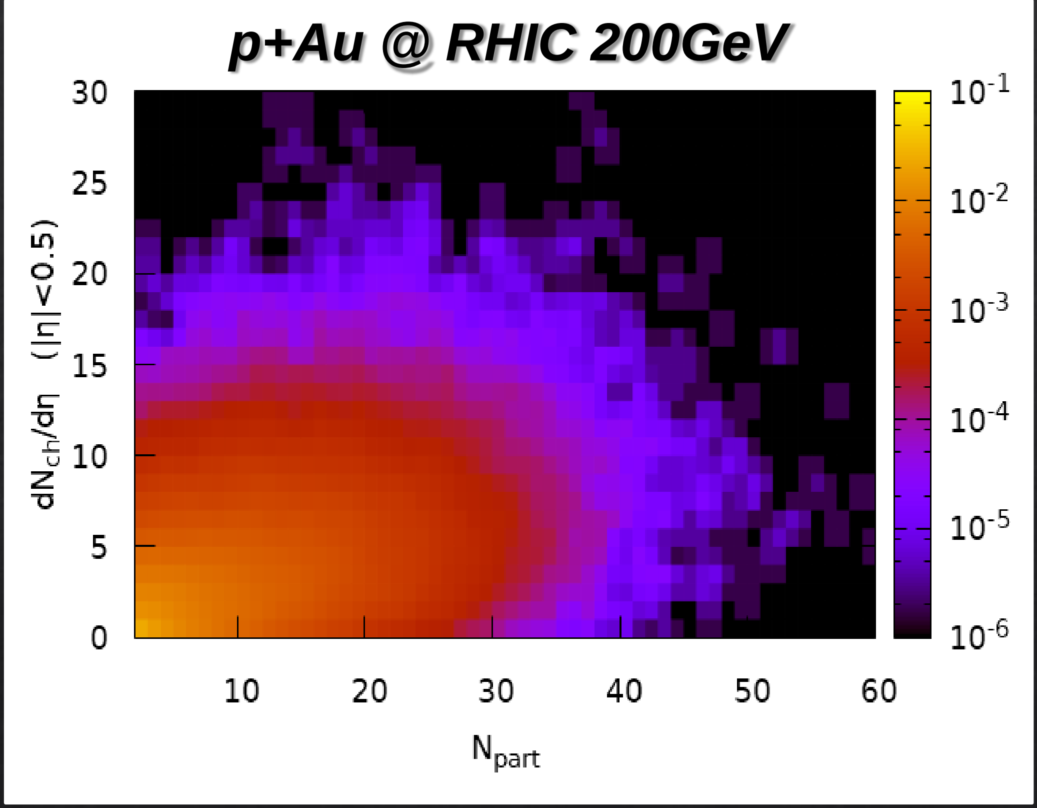

Correlation between participant number and charged particle multiplicity at midrapidity

BUT

large dispersion in both quantities in p+A respect to A+A collisions

Centrality in small systems

LO, Moreau, Voronyuk and Bratkovskaya, 1909.06770

Miller *et al.*, ARNPS 57 (2007) 205

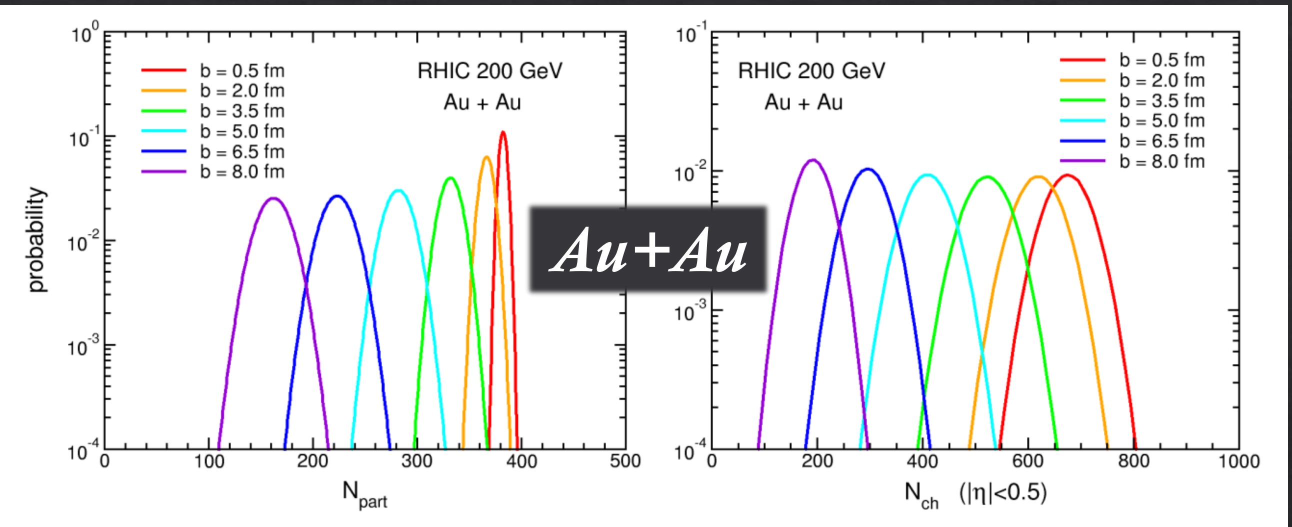

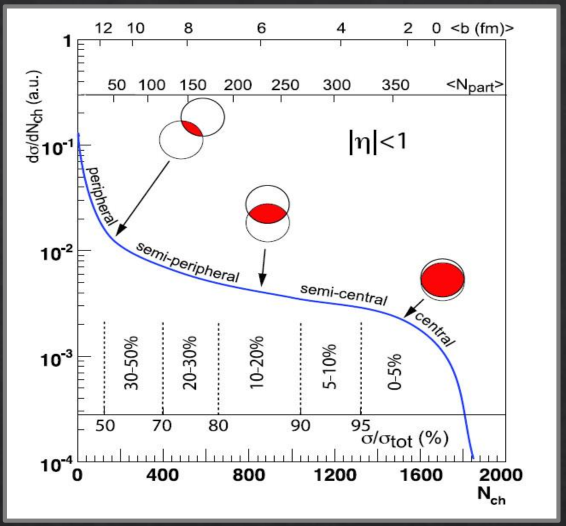

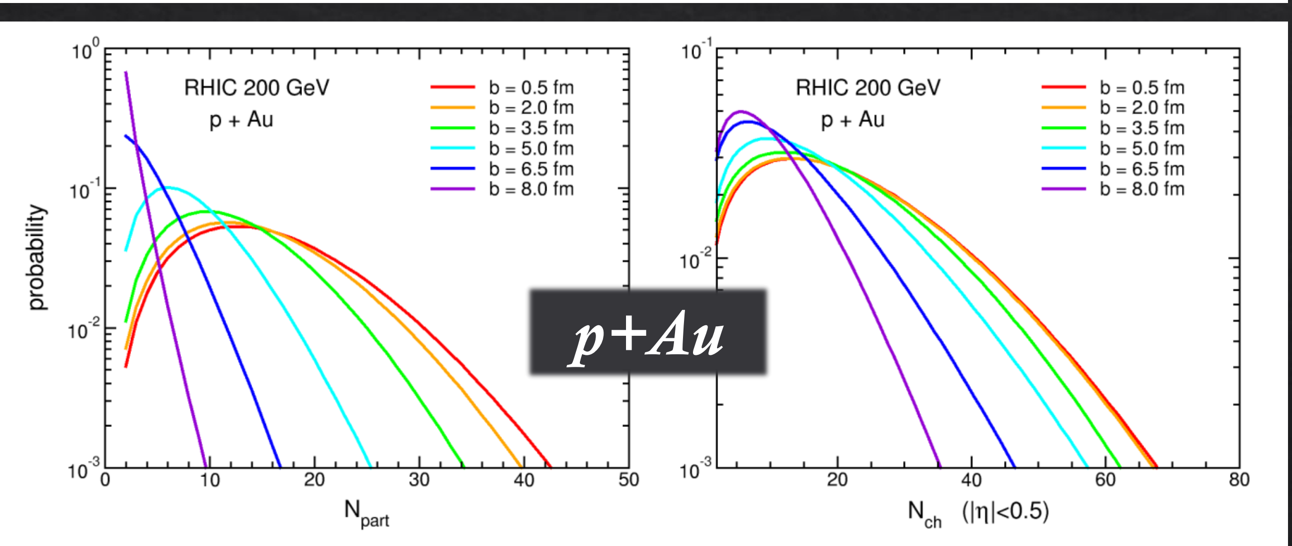

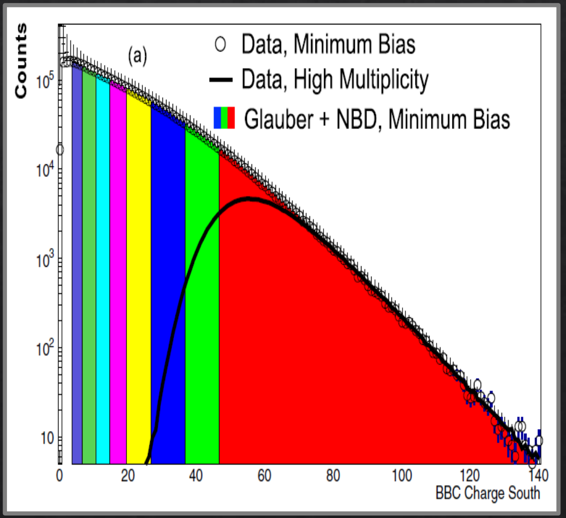

PHENIX, PRC 95 (2017) 034910

Multiplicity fluctuation in the final state mixes events from different impact parameters!

p+Au: rapidity distributions

Exp. Data: PHENIX Collaboration, PRL 121 (2018) 222301

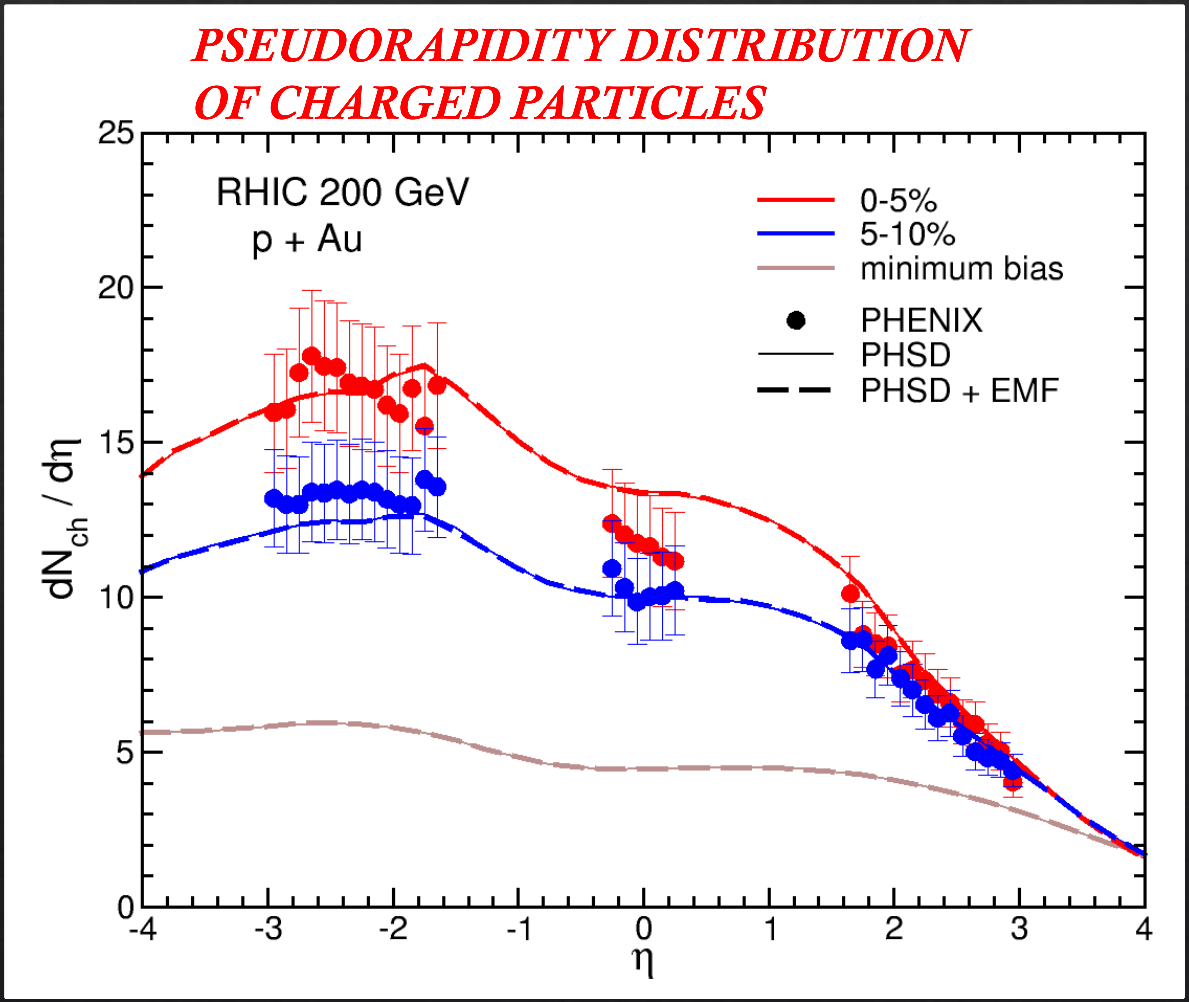

LO, Moreau, Voronyuk and Bratkovskaya, 1909.06770

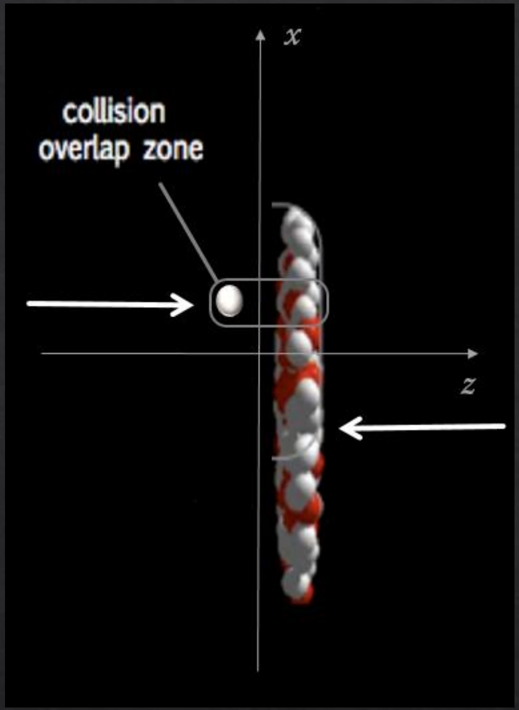

- enhanced particle production in the Au-going directions
- asymmetry increases with centrality of the collision

p+Au: rapidity distributions

RAPIDITY DISTRIBUTION OF IDENTIFIED PARTICLES

RHIC 200GeV
p+Au 0-5%

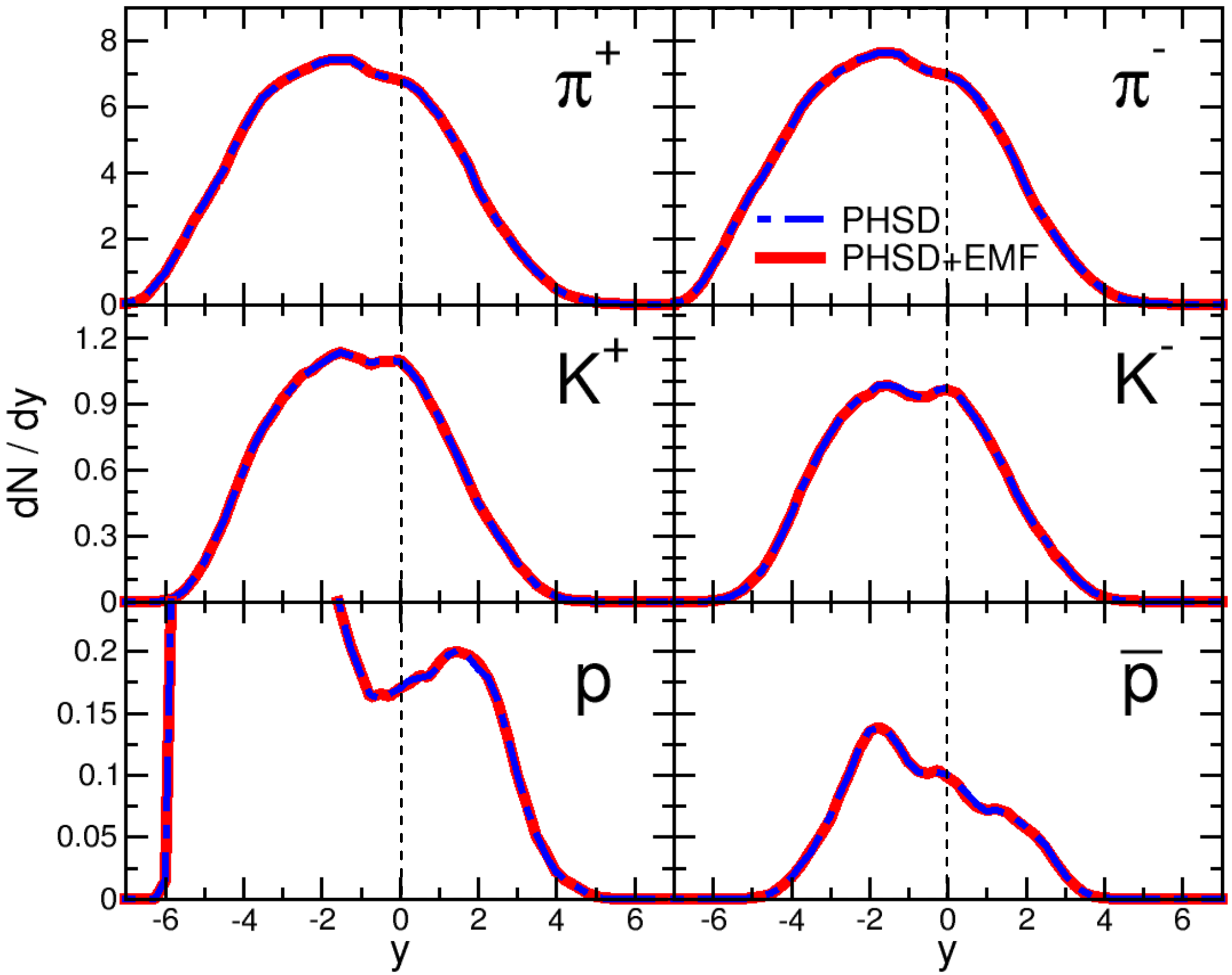

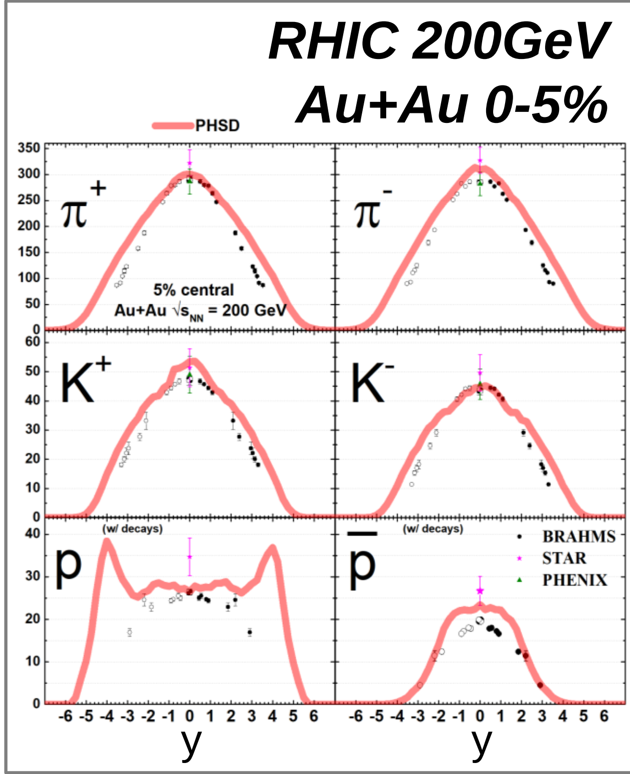

symmetric colliding system

LO, Moreau, Voronyuk and Bratkovskaya, 1909.06770

p+Au: rapidity distributions

RAPIDITY DISTRIBUTION OF IDENTIFIED PARTICLES
channel decomposition

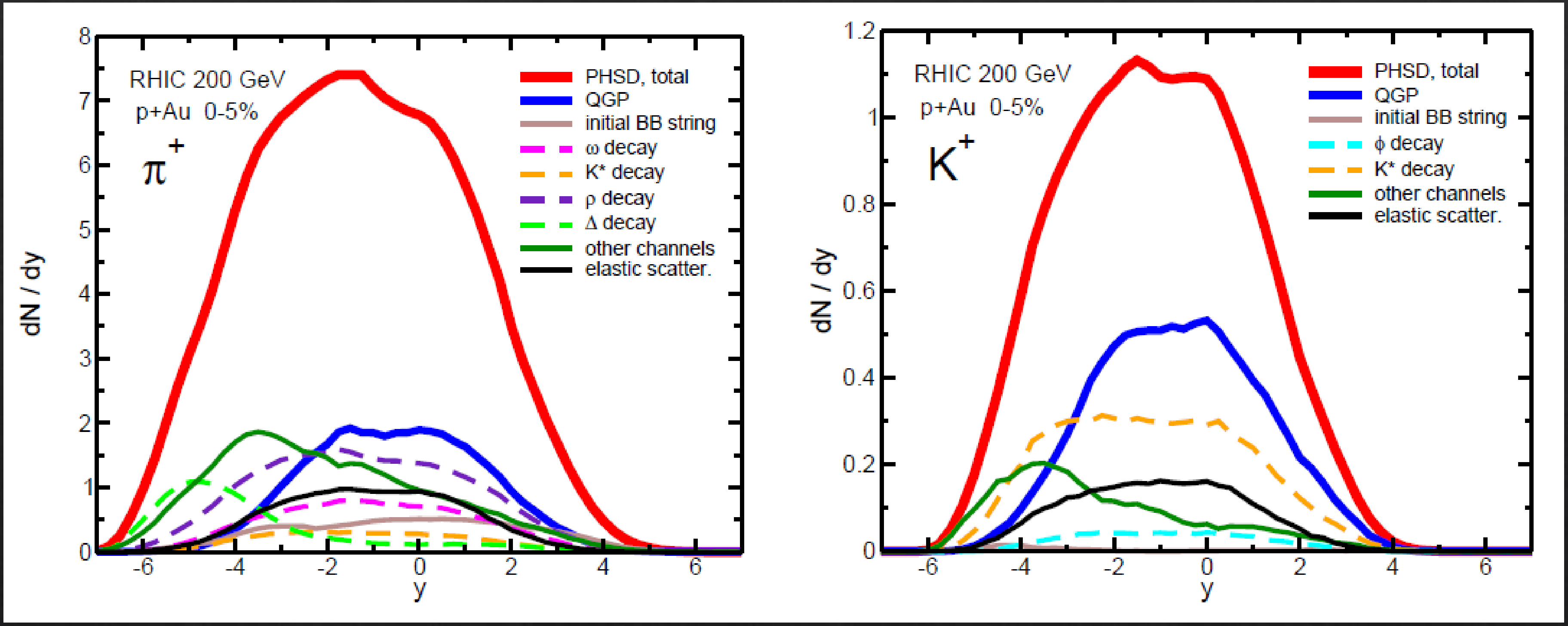

large amount of particles escapes from the medium just after production from QGP hadronization without further rescattering

Anisotropic radial flow

A DEEPER INSIGHT…INITIAL-STATE FLUCTUATIONS

Not a simple **almond shape**

- ➢ odd harmonics = 0

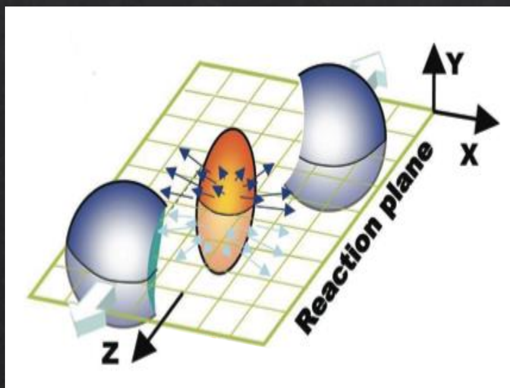

$$E\frac{d^3N}{d^3p}=\frac{1}{2\pi}\frac{d^2N}{p_T dp_T dy}\left(1+2\sum_{n=1}^{\infty}v_n(p_T,y)\cos\left(n\left(\phi-\Psi_r\right)\right)\right)$$

$$v_n=\left\langle\cos\left(n\left(\phi-\Psi_r\right)\right)\right\rangle$$

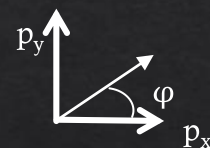

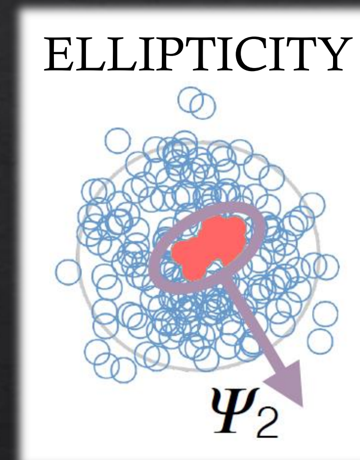

But a **"lumpy" profile due to fluctuations** of nucleon position in the overlap region

- ➢ odd harmonics ≠ 0

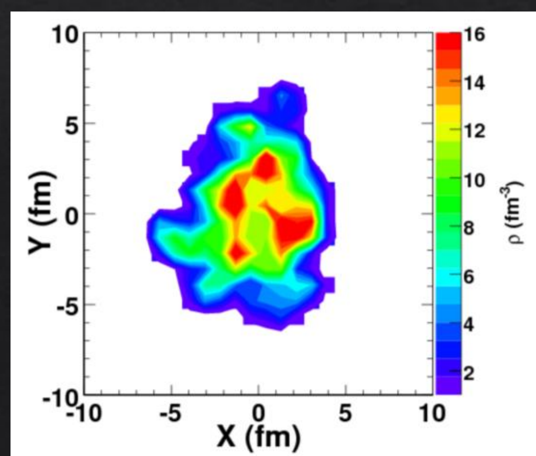

Plumari et al., PRC 92 (2015) 054902

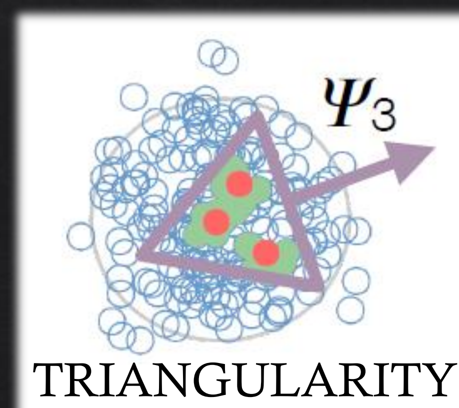

Anisotropic radial flow

A DEEPER INSIGHT…FINITE EVENT MULTIPLICITY

azimuthal particle distributions
w.r.t. the reaction plane

$$\frac{dN}{d\varphi} \propto 1 + \sum_n 2 v_n(p_T) \cos[n(\varphi - \Psi_n)]$$

n-th order
flow harmonics

$$v_n = \frac{\langle \cos[n(\varphi - \Psi_n)] \rangle}{Res(\Psi_n)}$$

event-plane angle resolution
(three-subevent method)

n-th order
event-plane angle

$$\Psi_n = \frac{1}{n} \operatorname{atan2}(Q_n^y, Q_n^x)$$

$$Q_n^x = \sum_i \cos[n\varphi_i]$$

$$Q_n^y = \sum_i \sin[n\varphi_i]$$

Since the finite number of particles produces limited resolution in the determination of Ψ_n, the v_n must be corrected up to what they would be relative to the real reaction plane

Poskanzer and Voloshin,
PRC 58 (1998) 1671

Important especially for small colliding system, e.g. p+A

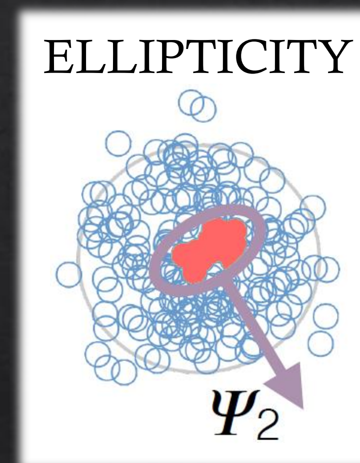

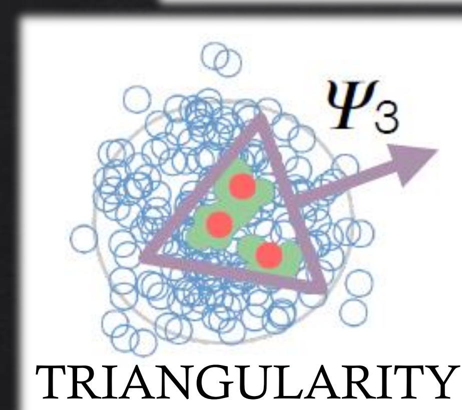

p+Au: elliptic flow

ELLIPTIC FLOW OF CHARGED PARTICLES

$$v_2(p_T) = \frac{\langle \cos[2(\varphi(p_T) - \Psi_2)] \rangle}{Res(\Psi_2)}$$

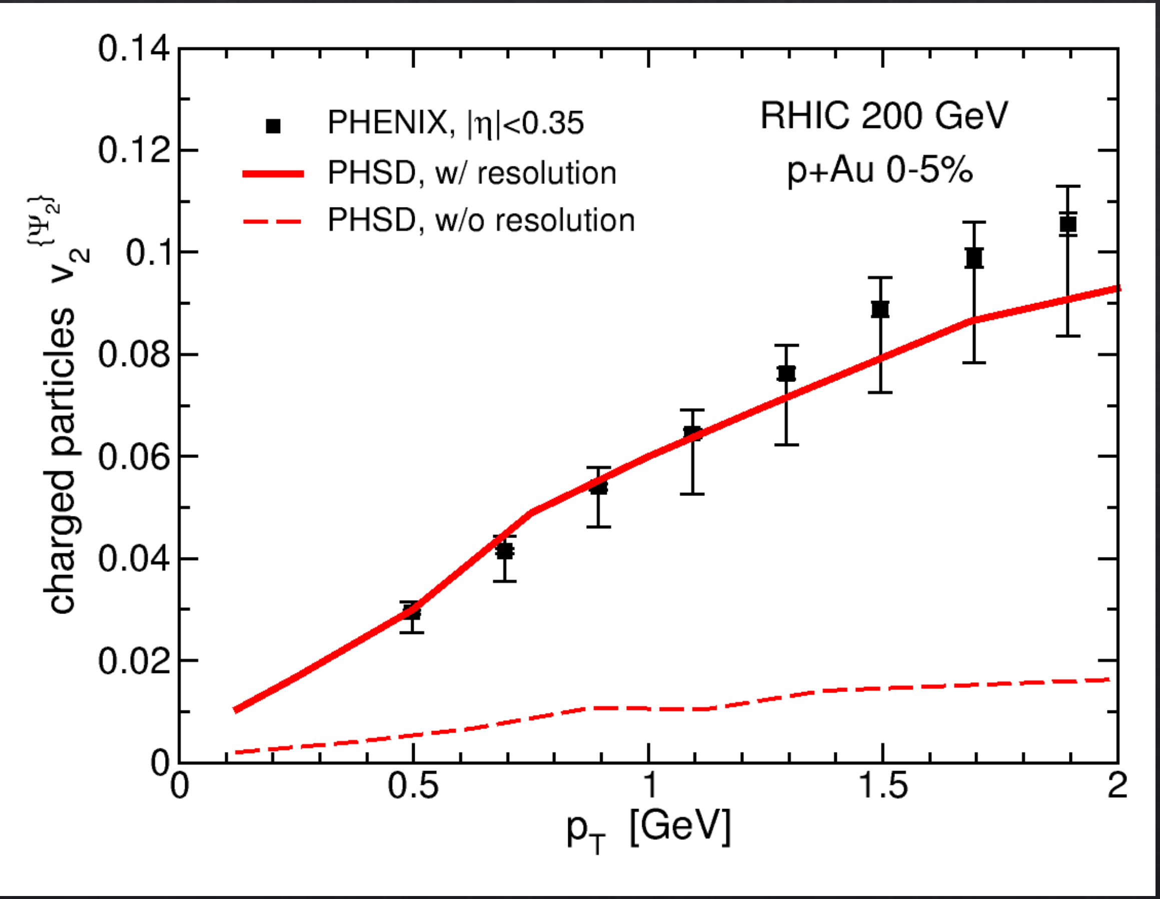

Event-plane angle in $-3 < \eta < -1$:
$Res(\Psi_2^{PHSD}) = 0.175$
$Res(\Psi_2^{PHENIX}) = 0.171$

magnitude correlated with the determination of the reaction plane

LO, Moreau, Voronyuk and Bratkovskaya, 1909.06770
Exp. data: Aidala et al. (PHENIX Collaboration), PRC 95 (2017) 034910

p+Au: elliptic flow

ELLIPTIC FLOW OF CHARGED PARTICLES

$$v_2(p_T) = \frac{\langle \cos[2(\varphi(p_T) - \Psi_2)] \rangle}{Res(\Psi_2)}$$

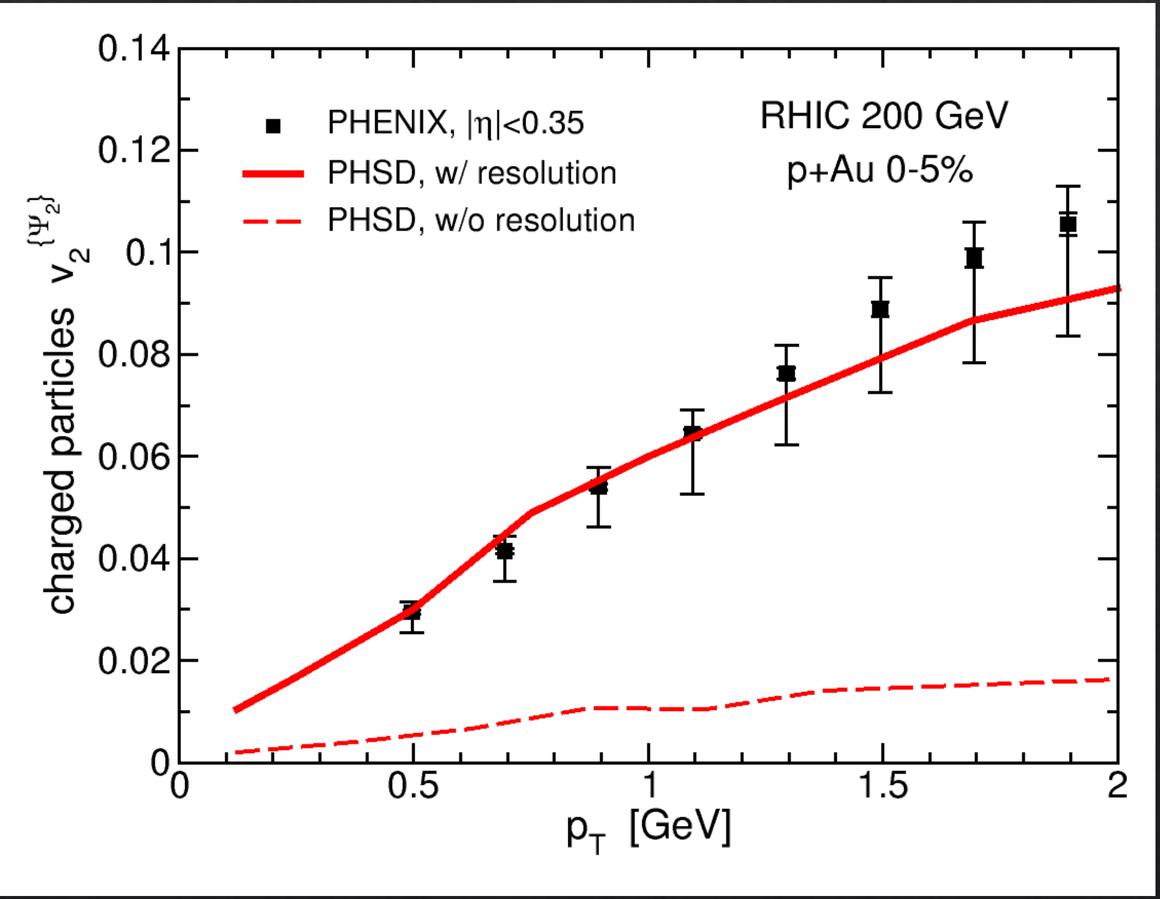

LO, Moreau, Voronyuk and Bratkovskaya, 1909.06770

Exp. data: Aidala et al. (PHENIX Collaboration), PRC 95 (2017) 034910

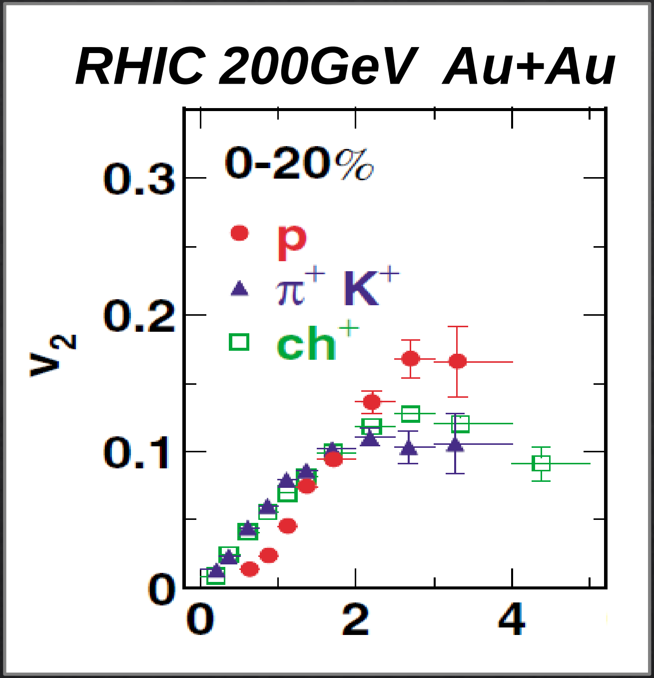

PHENIX, PRL 91 (2003) 182301

comparable to that found in large colliding systems

p+Au: directed flow

pseudorapidity dependence of the
DIRECTED FLOW OF CHARGED PARTICLES

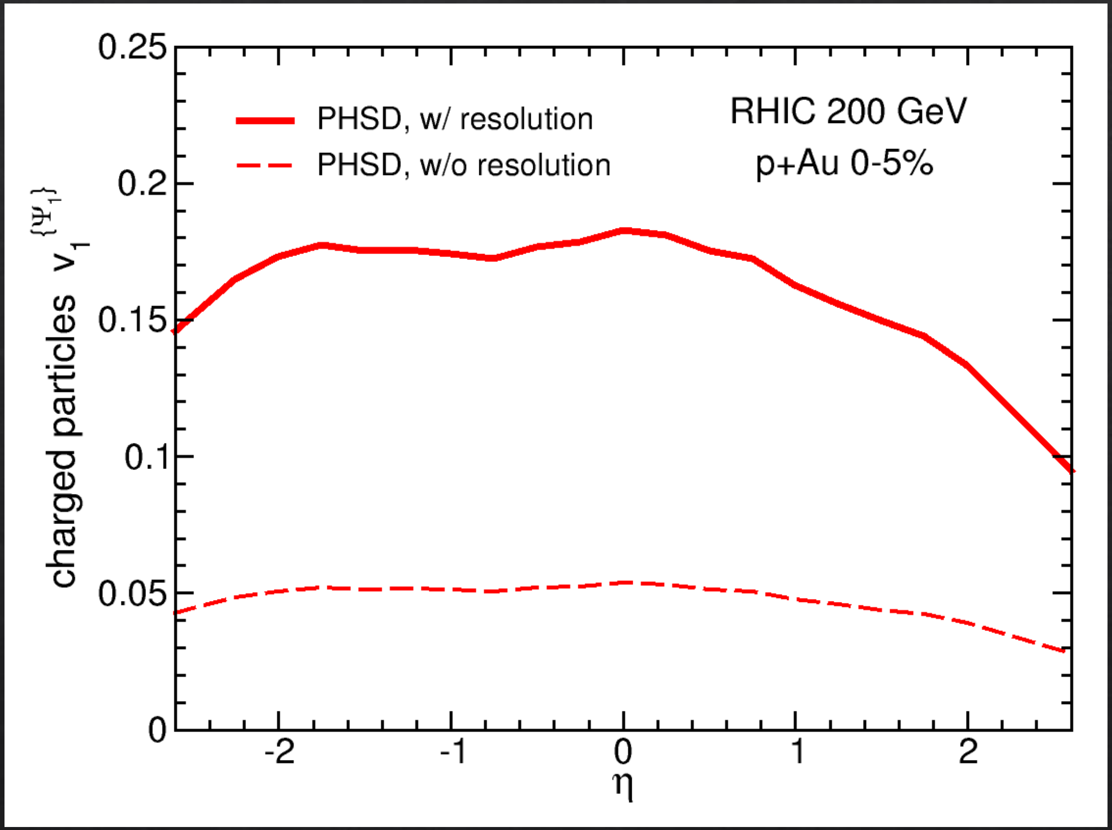

LO, Moreau, Voronyuk and Bratkovskaya, 1909.06770

$$v_1(\eta) = \frac{\langle \cos[\varphi(\eta) - \Psi_1] \rangle}{Res(\Psi_1)}$$

Event-plane angle in $-4 < \eta < -3$: $Res(\Psi_1^{PHSD}) = 0.397$

magnitude correlated with the determination of the reaction plane

p+Au: directed flow

pseudorapidity dependence of the
DIRECTED FLOW OF CHARGED PART

STAR Collaboration, PRL 101 (2008) 252301

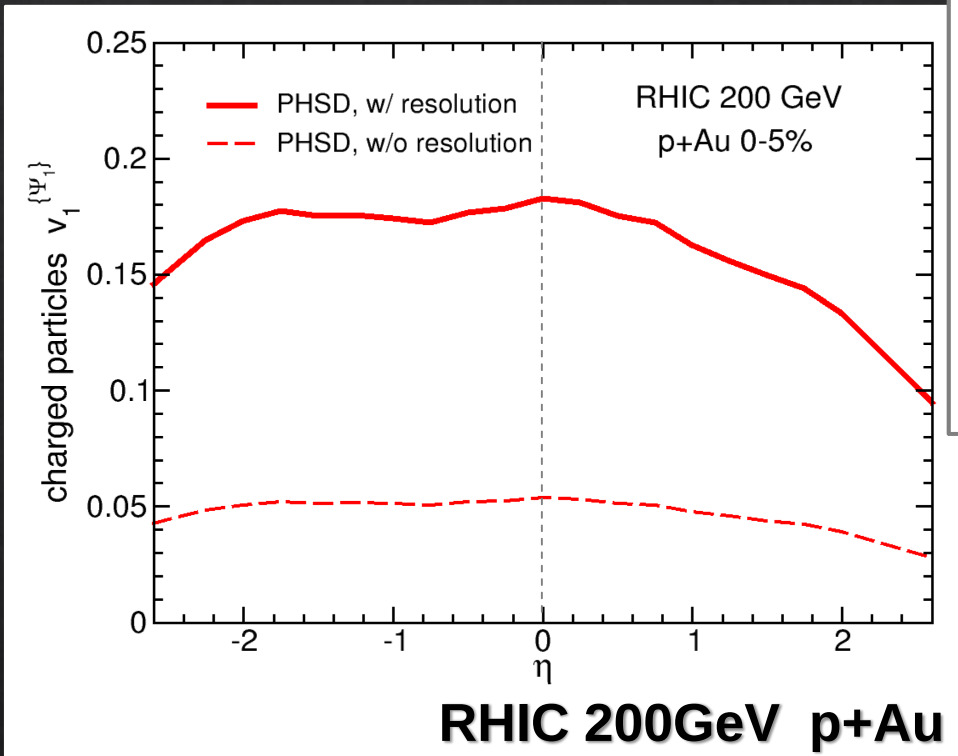

LO, Moreau, Voronyuk and Bratkovskaya, 1909.06770

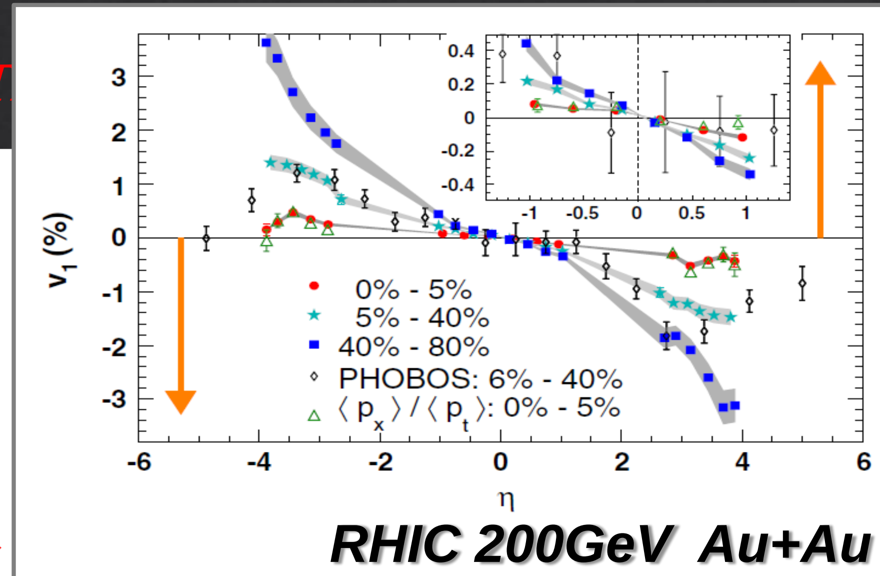

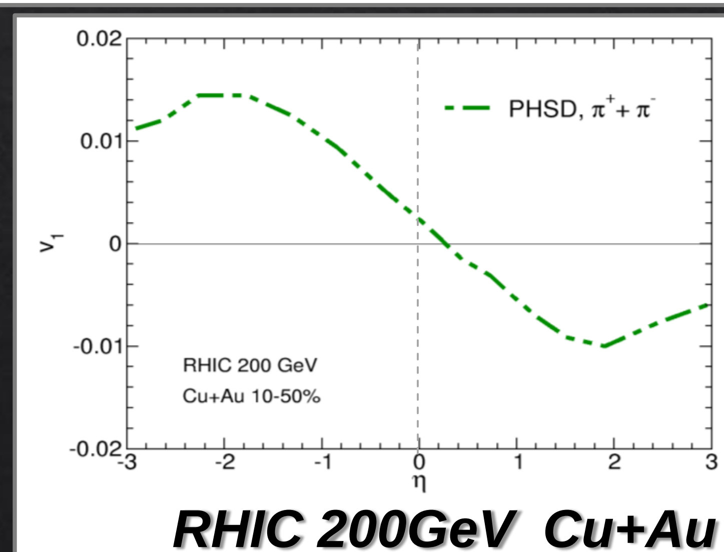

Voronyuk *et al.*, PRC 90 (2014) 064903
Toneev *et al.*, PRC 95 (2017) 034911

p+Au: directed flow

pseudorapidity dependence of the
DIRECTED FLOW OF CHARGED PARTICLES

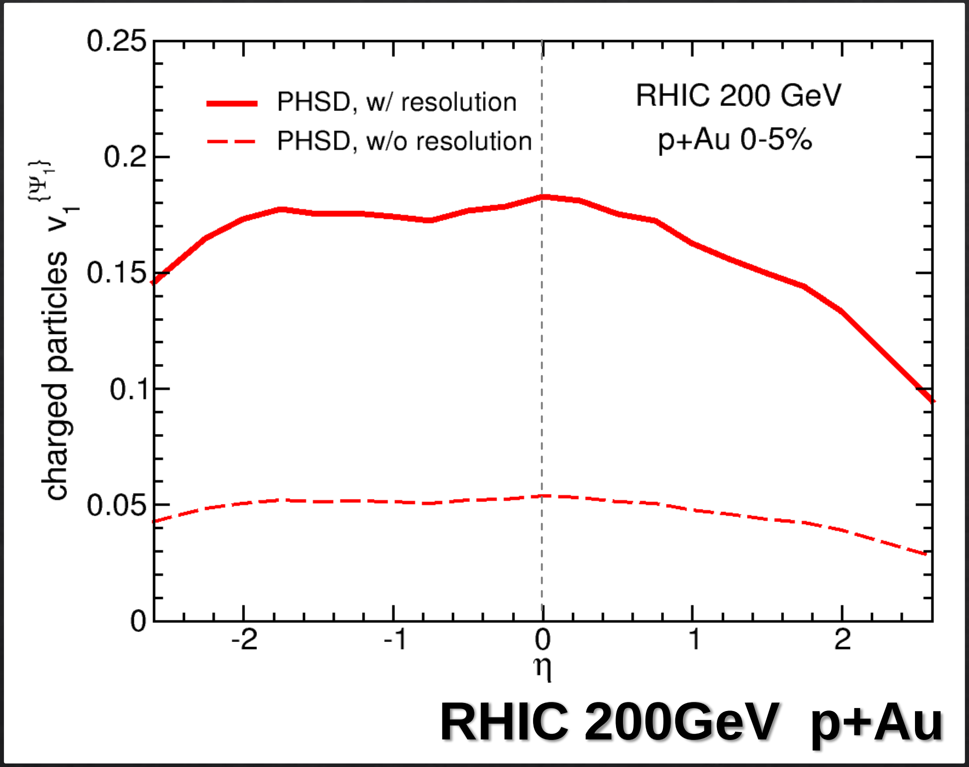

LO, Moreau, Voronyuk and Bratkovskaya, 1909.06770

SPLITTING OF POSITIVELY AND NEGATIVELY CHARGED PARTICLES INDUCED BY THE ELECTROMAGNETIC FIELD?

p+Au: directed flow

rapidity dependence of the
DIRECTED FLOW OF IDENTIFIED PARTICLES

$$v_1(\eta) = \frac{\langle \cos[\varphi(\eta) - \Psi_1] \rangle}{Res(\Psi_1)}$$

LO, Moreau, Voronyuk and Bratkovskaya, 1909.06770

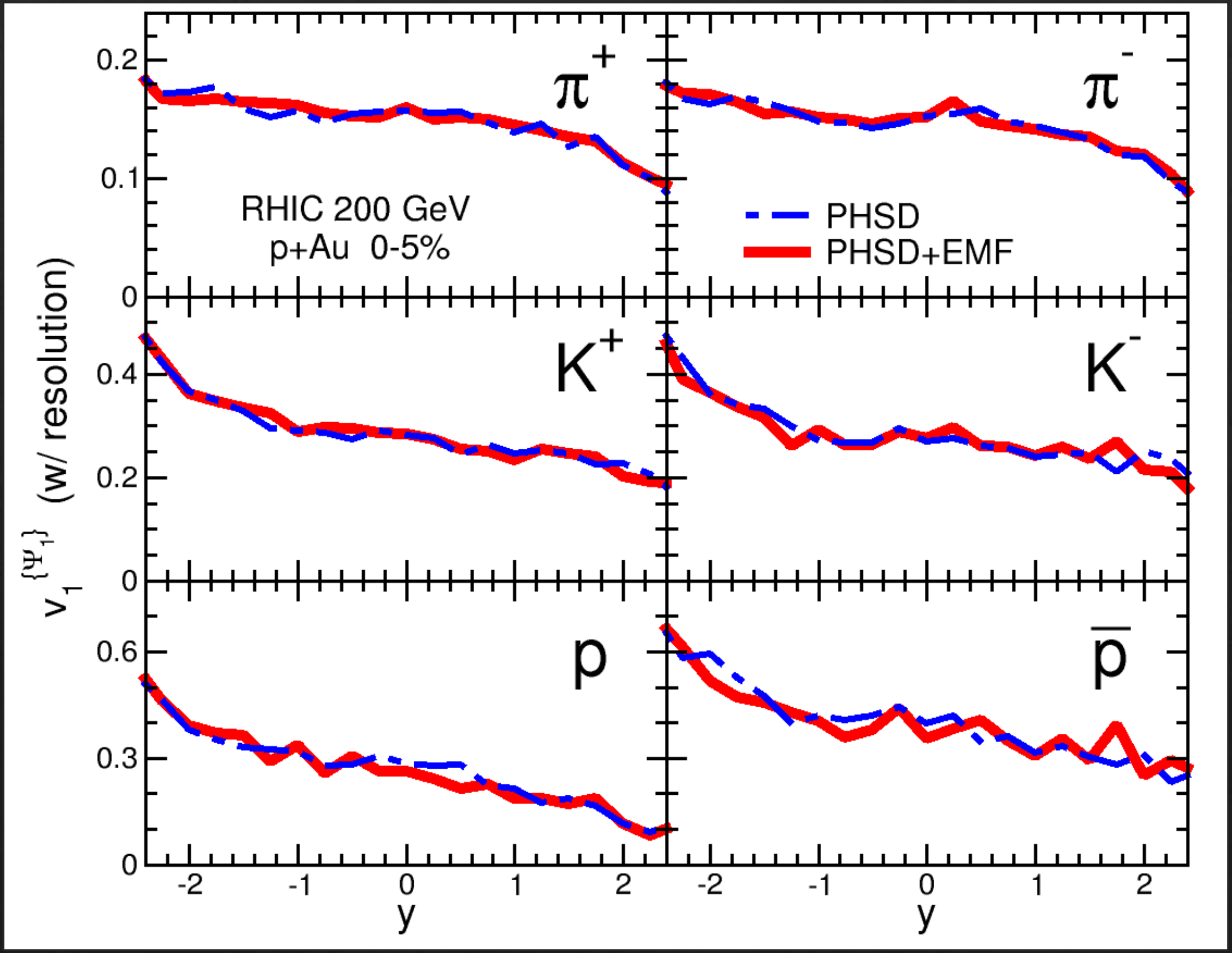

SPLITTING INDUCED BY THE EM FIELD?

no visible changes with and without electromagnetic fields for 5% central collisions

BUT…

p+Au: directed flow

rapidity dependence of the
DIRECTED FLOW OF PIONS

$$v_1(y) = \langle \cos[\varphi(y)] \rangle$$

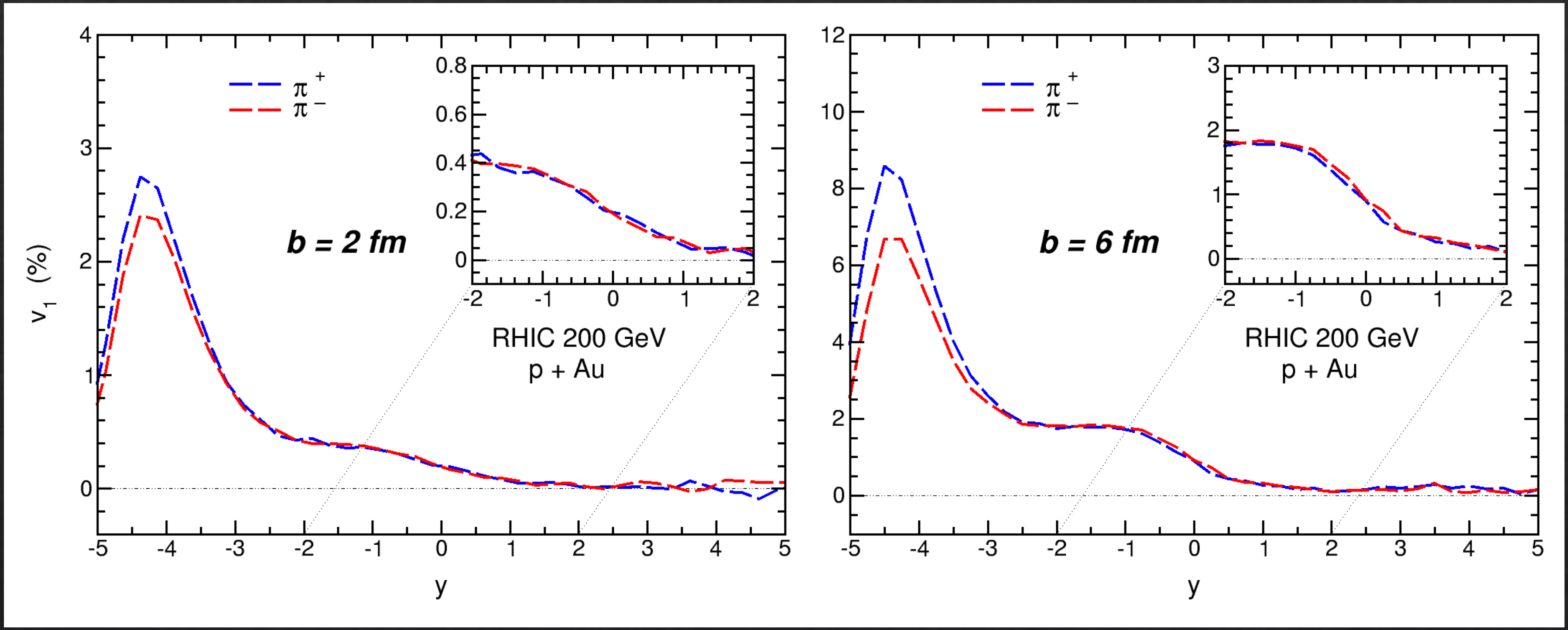

LO, Moreau, Voronyuk and Bratkovskaya, 1909.06770

SPLITTING INDUCED BY THE EM FIELD?

p+Au: directed flow

rapidity dependence of the
DIRECTED FLOW OF PIONS

$$v_1(y) = \langle \cos[\varphi(y)] \rangle$$

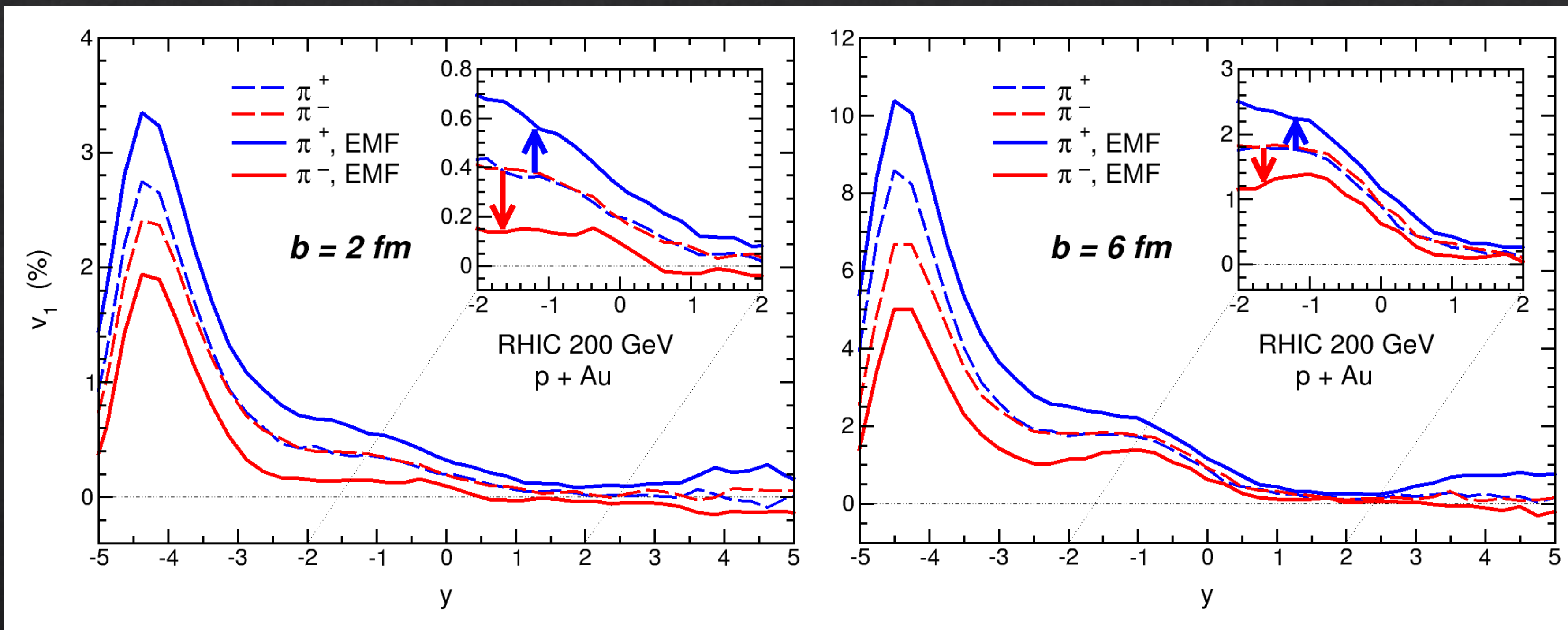

LO, Moreau, Voronyuk and Bratkovskaya, 1909.06770

Splitting of π^+ and π^- induced by the electromagnetic field

p+Au: directed flow

rapidity dependence of the
DIRECTED FLOW OF PIONS

collective sidewards deflection of particles

$$v_1 = \langle \cos\varphi \rangle = \langle p_x / p_T \rangle$$

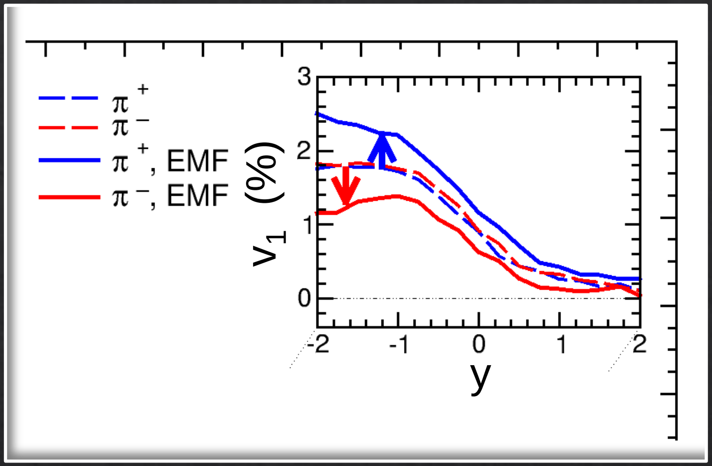

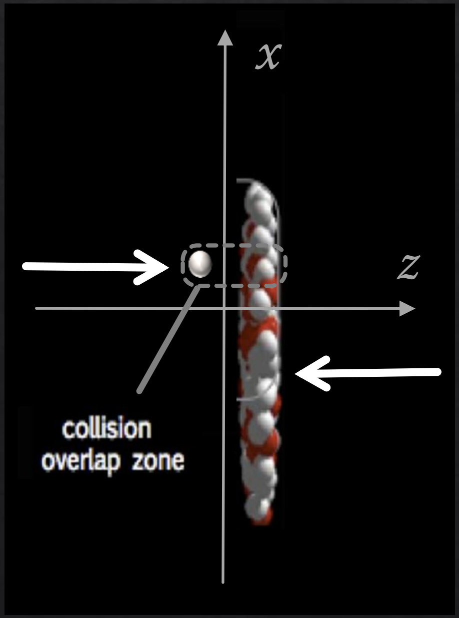

p+Au: directed flow

rapidity dependence of the
DIRECTED FLOW OF PIONS

collective sidewards deflection of particles

$$v_1 = \langle \cos\varphi \rangle = \langle p_x / p_T \rangle$$

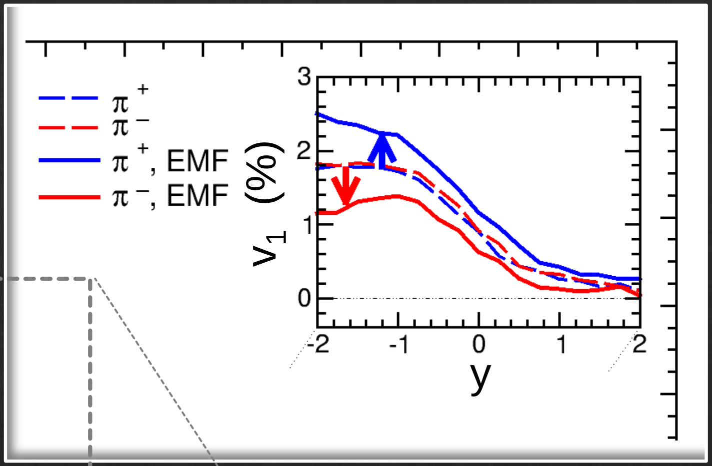

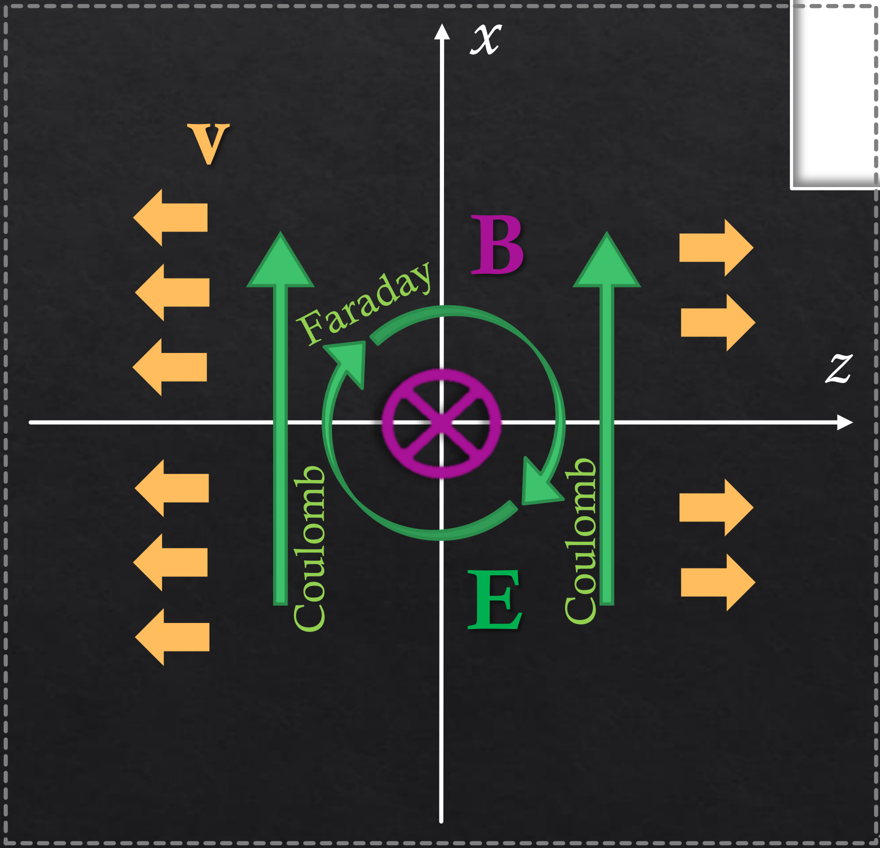

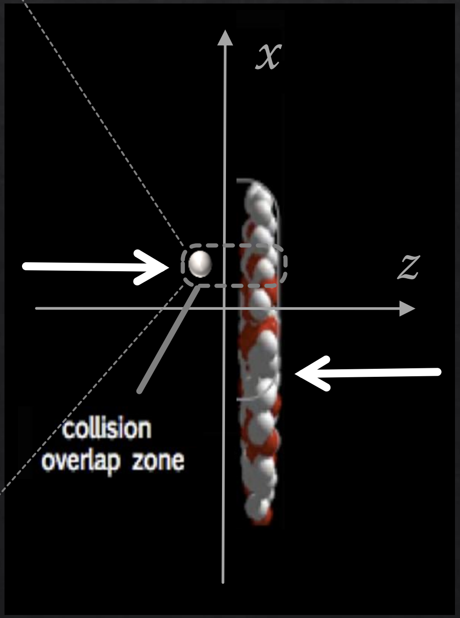

p+Au: directed flow

rapidity dependence of the
DIRECTED FLOW OF PIONS

collective sidewards deflection of particles

$$v_1 = \langle \cos\varphi \rangle = \langle p_x / p_T \rangle$$

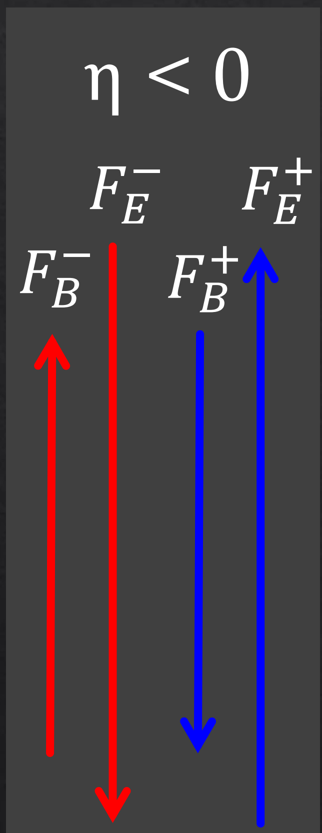

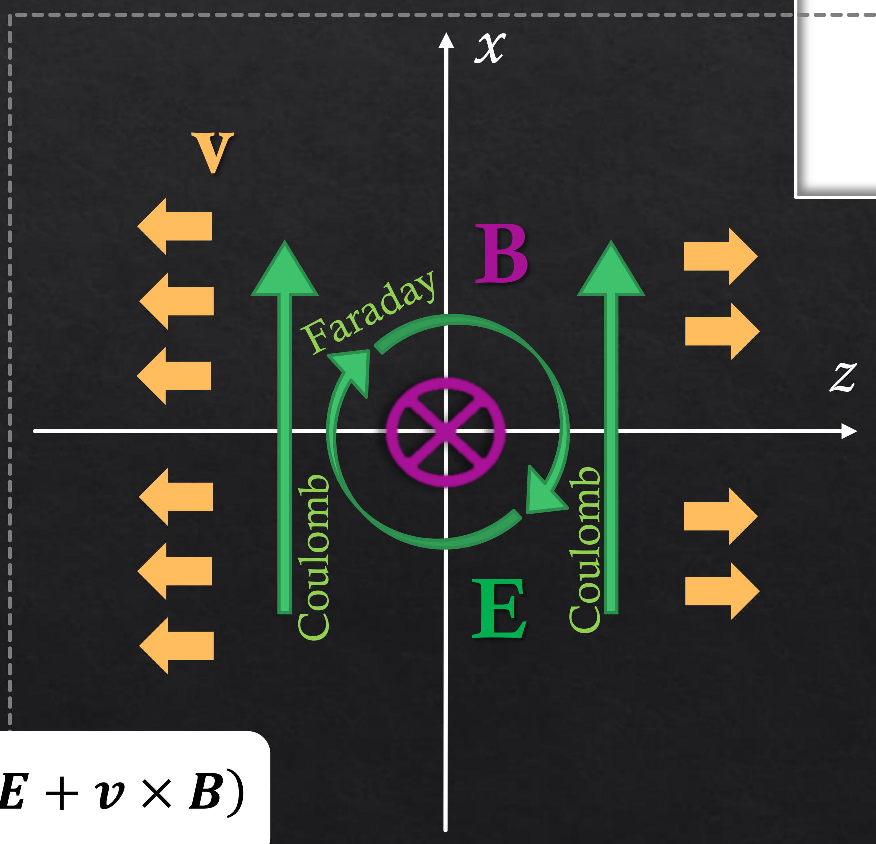

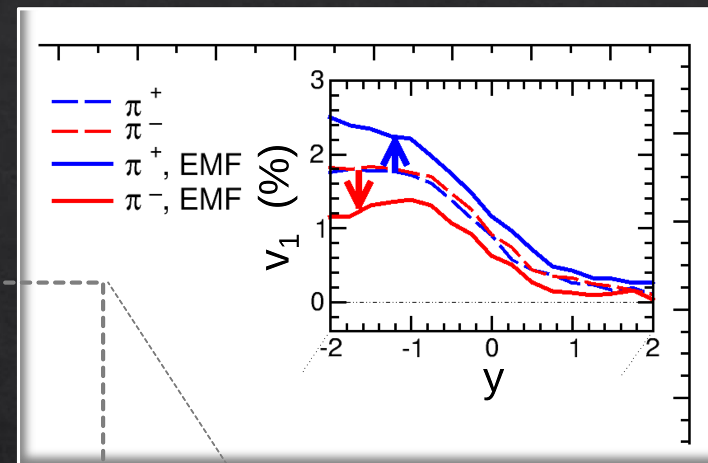

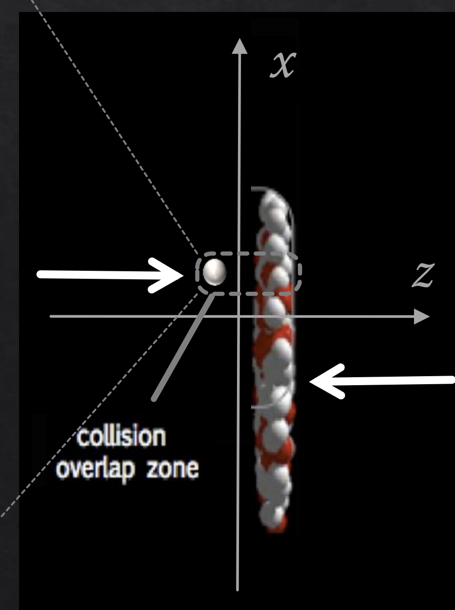

$$\boldsymbol{F}_{\boldsymbol{Lorentz}} = q(\boldsymbol{E} + \boldsymbol{v} \times \boldsymbol{B})$$

p+Au: directed flow

rapidity dependence of the
DIRECTED FLOW OF PIONS

$v_1(y) = \langle \cos[\varphi(y)] \rangle$

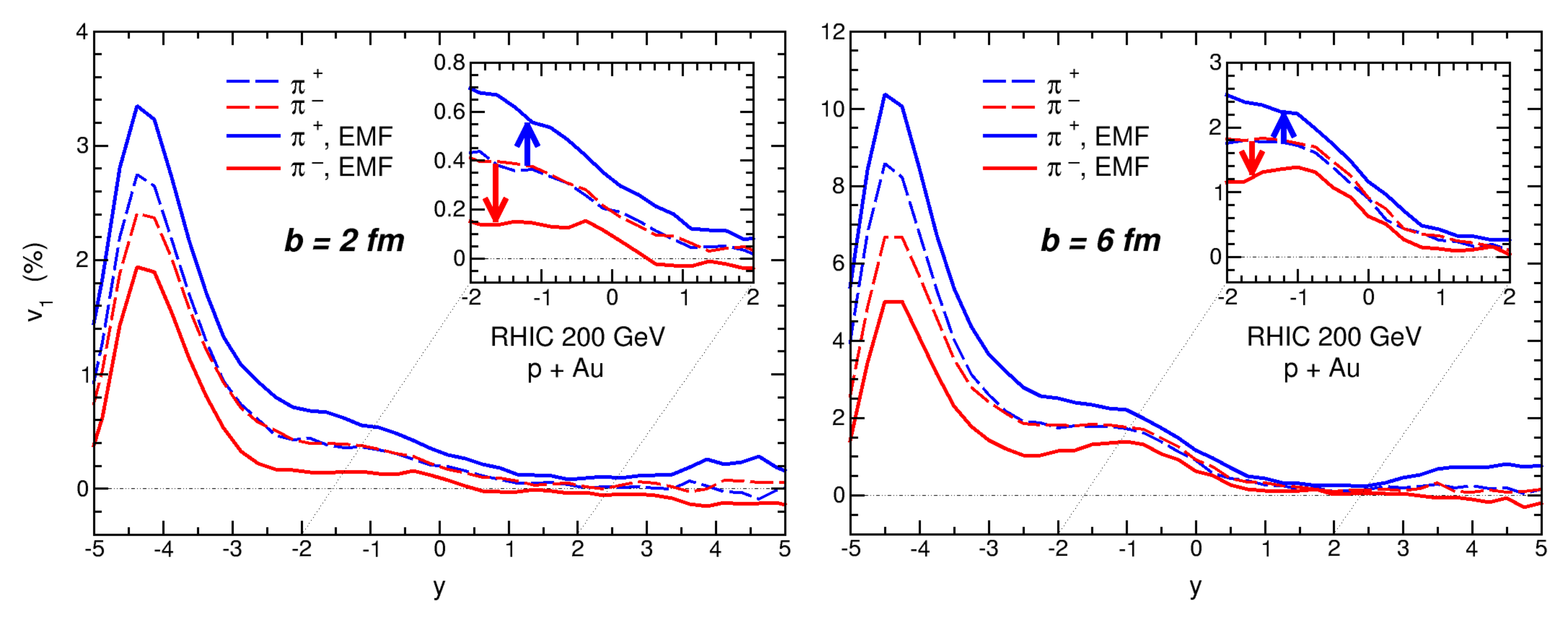

LO, Moreau, Voronyuk and Bratkovskaya

Splitting of π^+ and π^- induced by the electromagnetic field

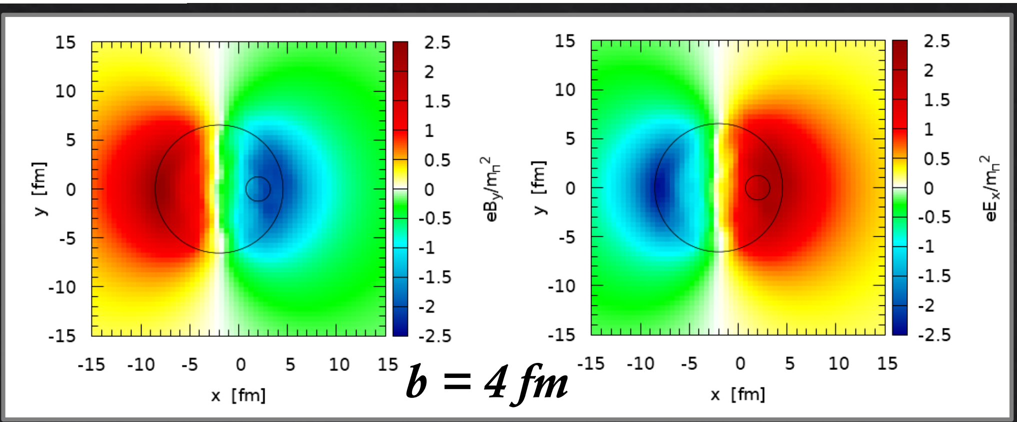

p+Au: directed flow

rapidity dependence of the
DIRECTED FLOW OF KAONS

$$v_1(y) = \langle \cos[\varphi(y)] \rangle$$

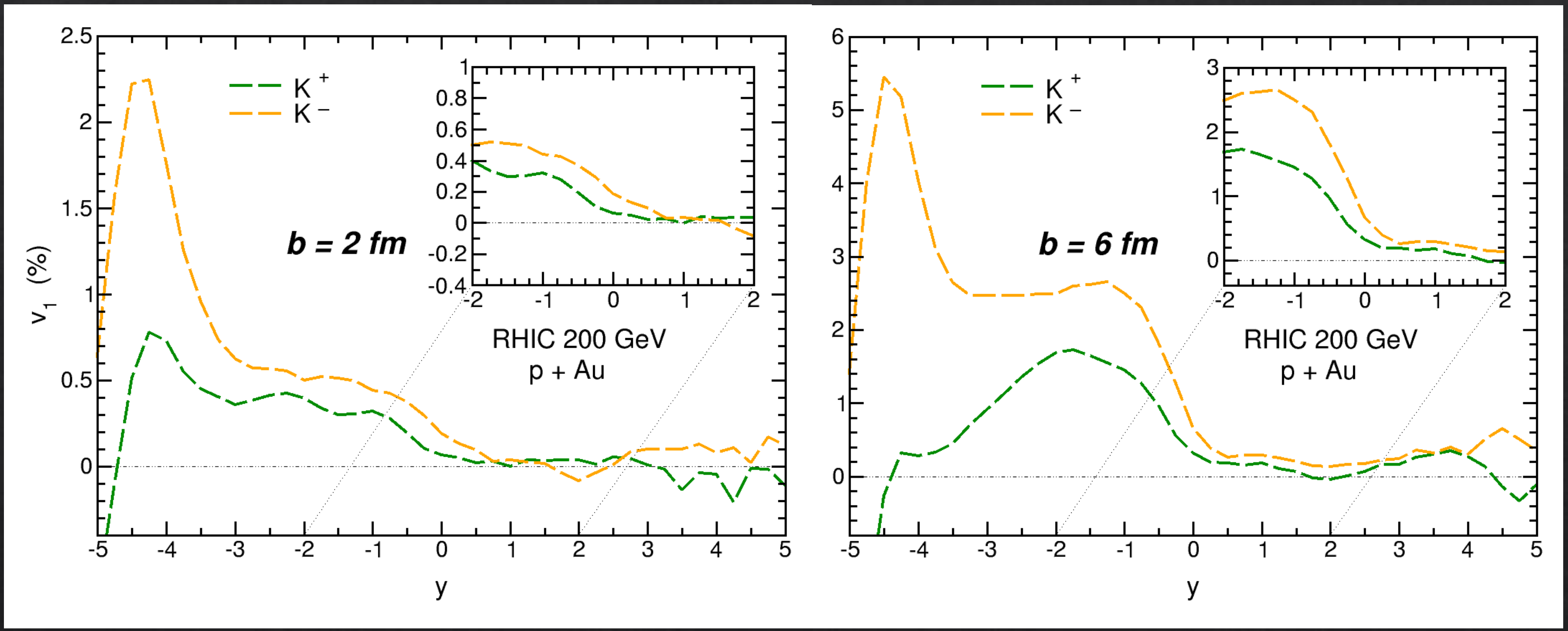

LO, Moreau, Voronyuk and Bratkovskaya, 1909.06770

p+Au: directed flow

rapidity dependence of the
DIRECTED FLOW OF KAONS

$$v_1(y) = \langle \cos[\varphi(y)] \rangle$$

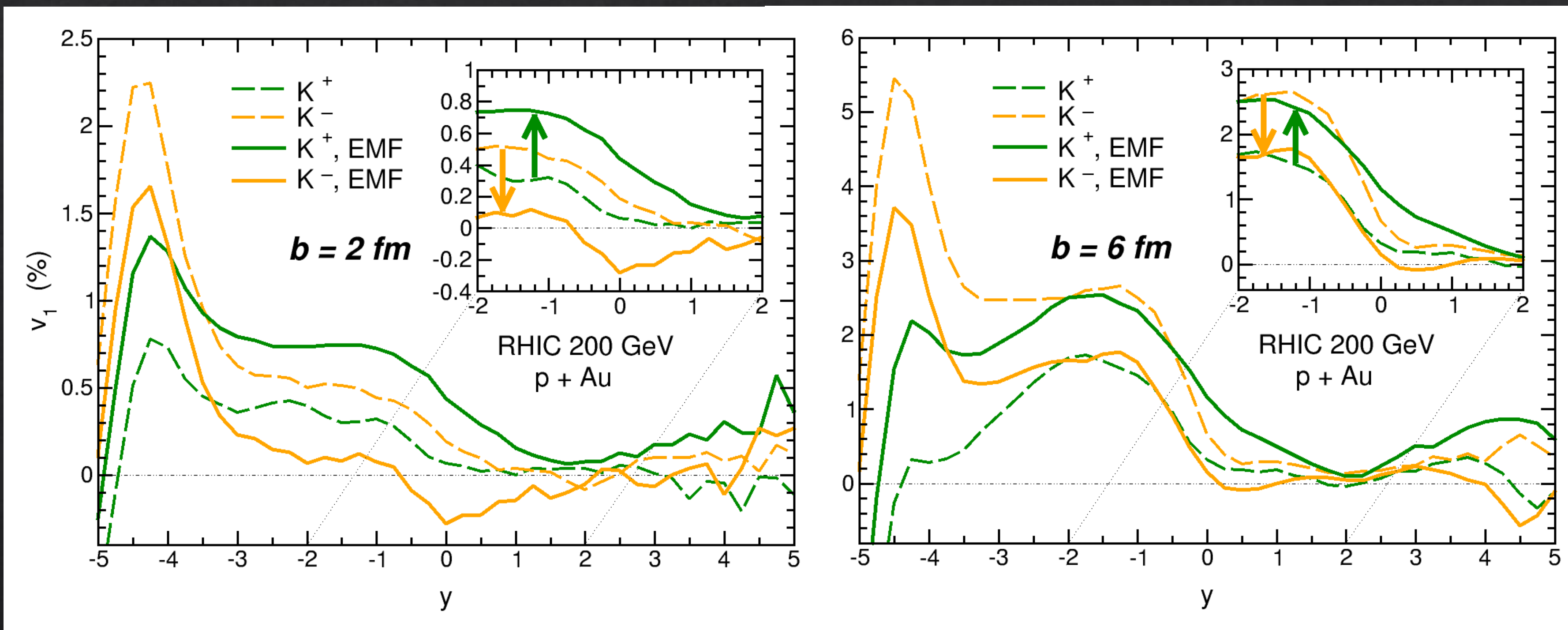

LO, Moreau, Voronyuk and Bratkovskaya

Splitting of K⁺ and K⁻ induced by the electromagnetic field

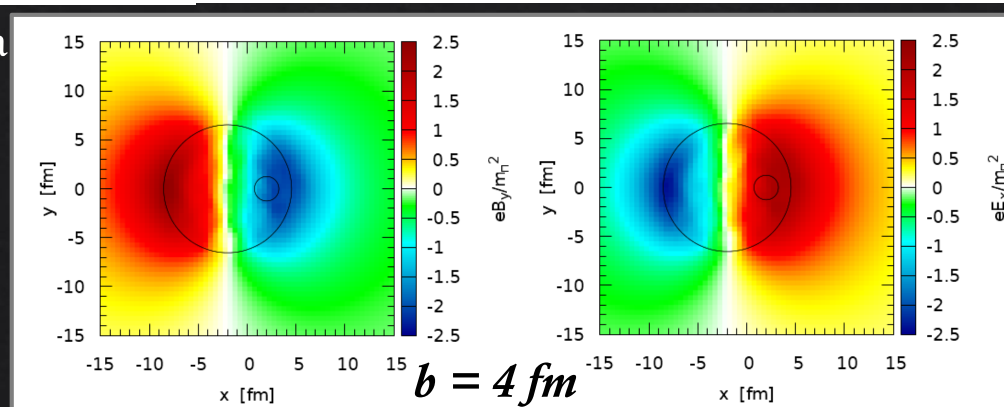

p+Au: directed flow

ELECTROMAGNETICALLY-INDUCED SPLITTING in the directed flow of hadrons with same mass and opposite charge

$$\Delta v_1{}^{emf} \equiv \Delta v_1{}^{(PHSD+EMF)} - \Delta v_1{}^{(PHSD)}$$

$$\Delta v_1 \equiv v_1^+ - v_1^-$$

LO, Moreau, Voronyuk and Bratkovskaya, 1909.06770

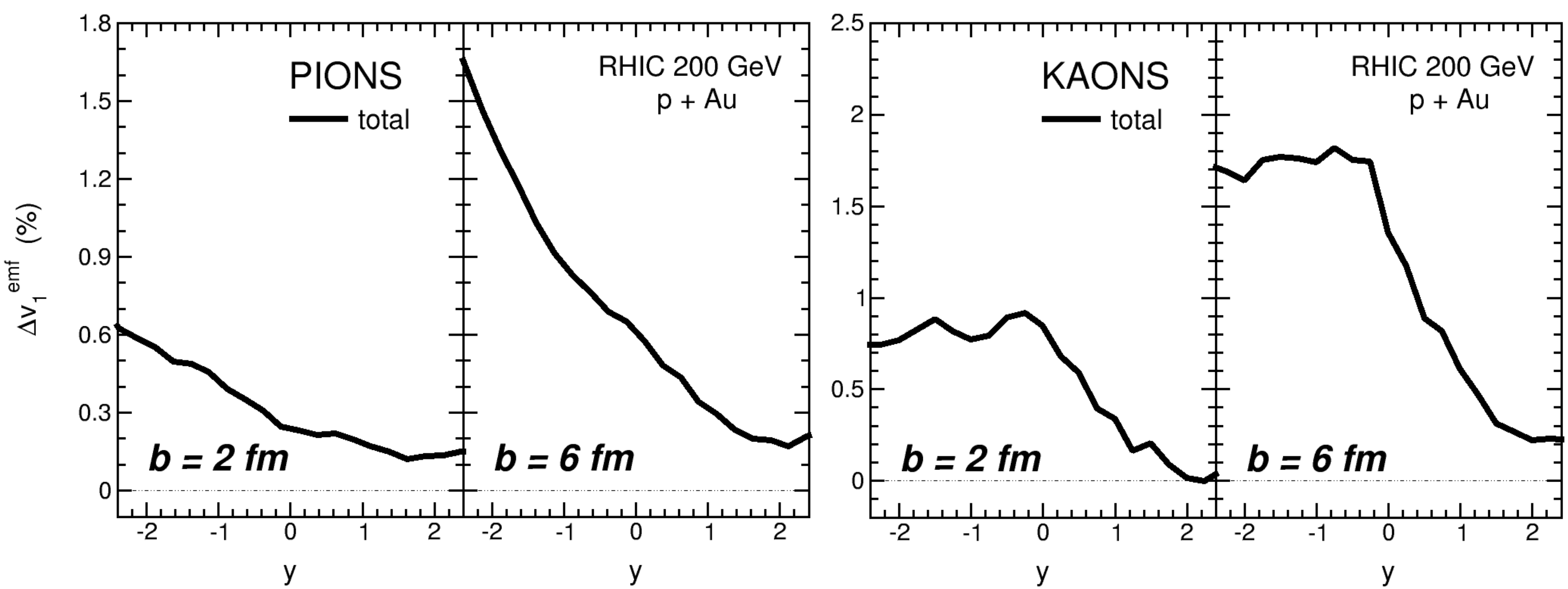

- **magnitude increasing with impact parameter**
- **larger splitting for kaons than for pions**

p+Au: directed flow

ELECTROMAGNETICALLY-INDUCED SPLITTING in the directed flow of hadrons with same mass and opposite charge

$$\Delta v_1^{emf} \equiv \Delta v_1^{(PHSD+EMF)} - \Delta v_1^{(PHSD)}$$

$$\Delta v_1 \equiv v_1^+ - v_1^-$$

LO, Moreau, Voronyuk and Bratkovskaya, 1909.06770

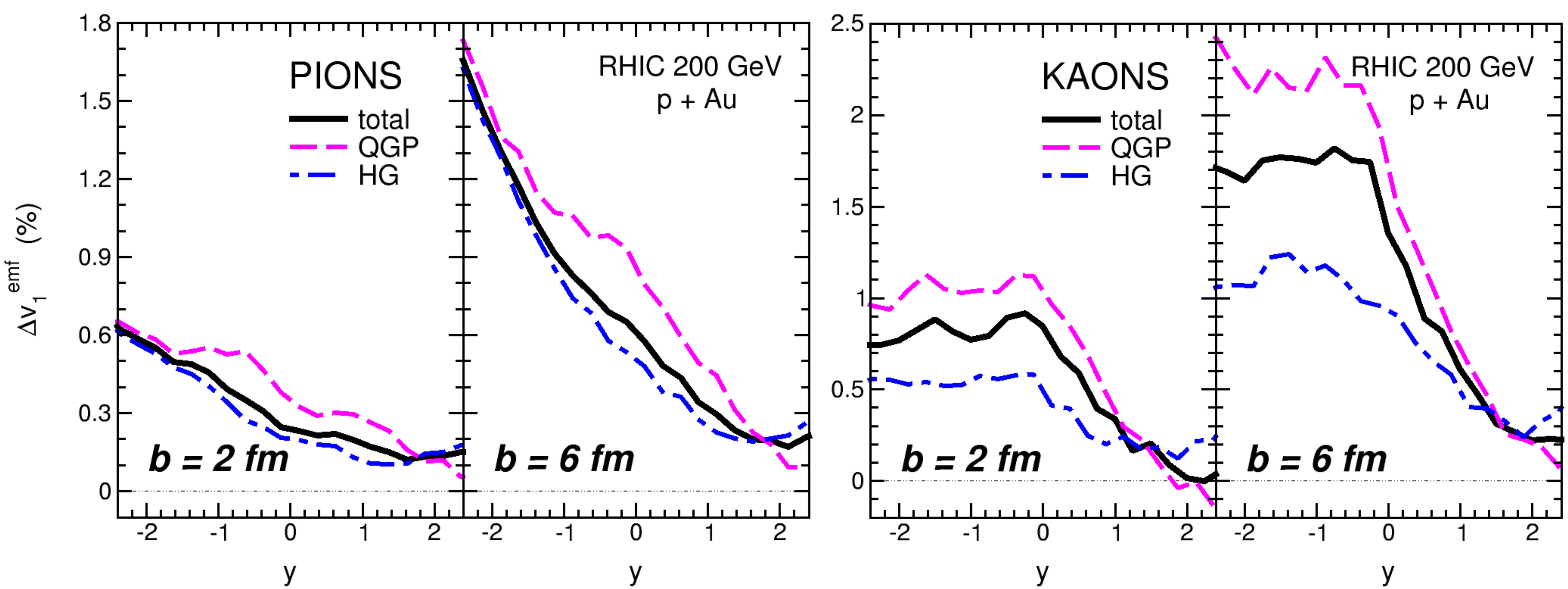

- **splitting generated at partonic level higher than that induced in the hadronic phase, especially for kaons**

CONCLUDING….

The Parton-Hadron-String-Dynamics (PHSD) approach describes the entire dynamical evolution of large and small colliding systems within one single theoretical framework

PHSD includes in a consistent way the intense electromagnetic fields produced in the very early stage of the collision

Study of p+Au collisions at top RHIC energy:

✓ the electric field is strongly asymmetric inside the overlap region

✓ asymmetry of charged-particle rapidity distributions increasing with centrality

✓ collectivity as signal of quark-gluon plasma formation

✓ effect of electromagnetic fields in directed flow of mesons: splitting between positively and negatively charged particle

✓ electromagnetically-induced splitting generated in the deconfined phase larger than that produced in the hadronic phase

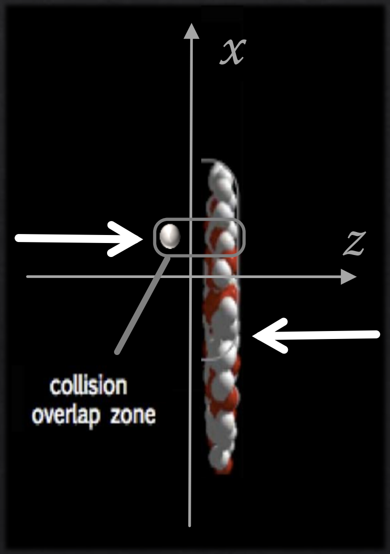

Thank you
for your attention!

p+Au collisions @ RHIC 200 GeV

Exp. Data: PHENIX Collaboration, PRL 121 (2018) 222

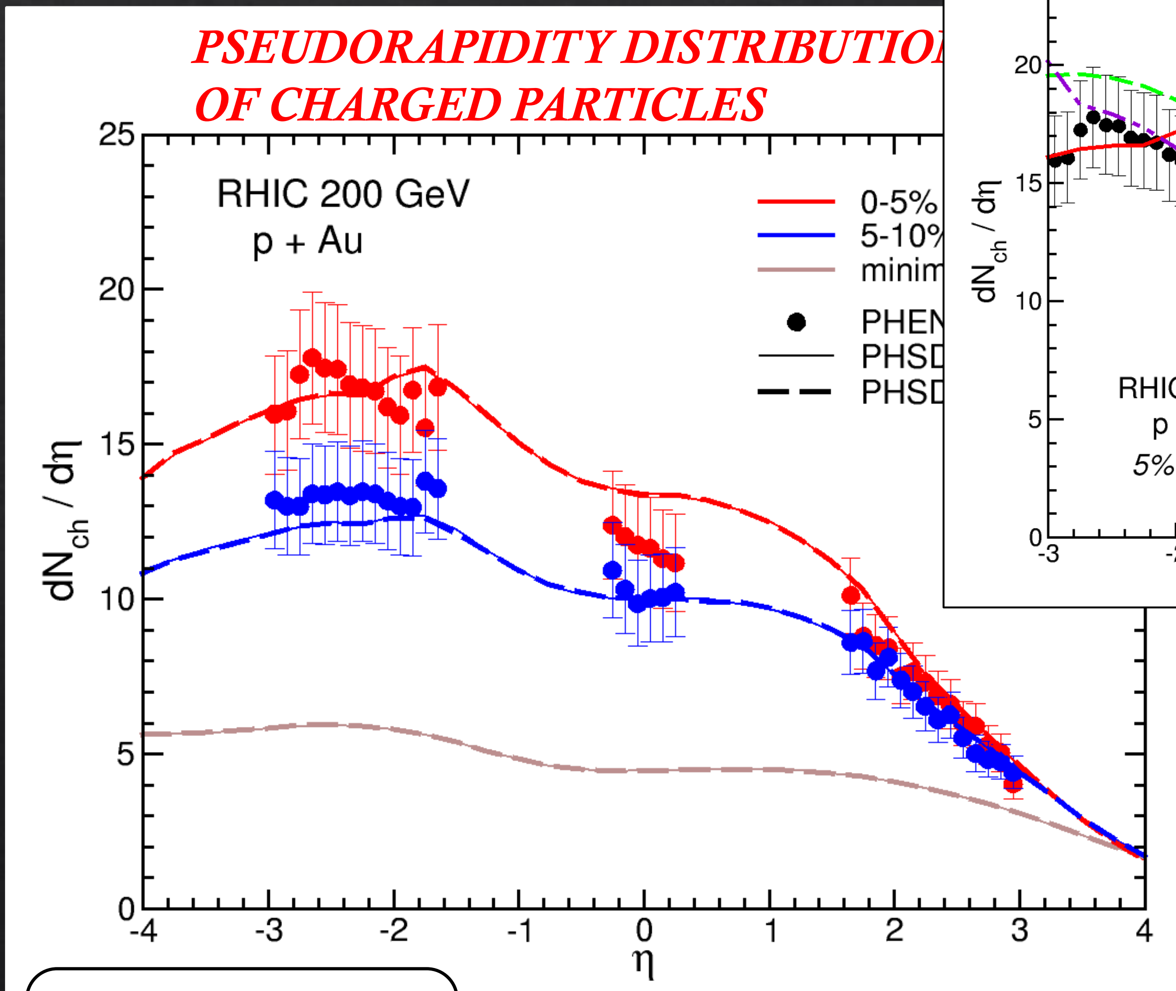

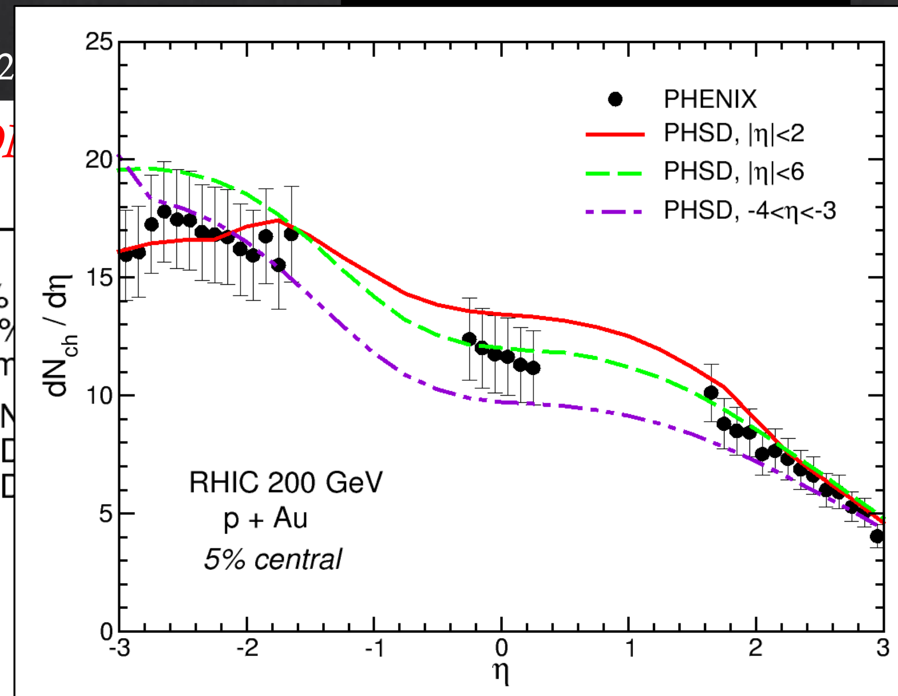

$$\eta = -\ln\left(\tan\frac{\theta}{2}\right)$$

- enhanced particle production in the Au-going directions
- asymmetry increases with centrality of the collision